R. & M. No. 2100
(5083)
A.R.C. Technical Report

MINISTRY OF SUPPLY

AERONAUTICAL RESEARCH COUNCIL
REPORTS AND MEMORANDA

Stress Concentration Due to Four-point Fixing at Front End of Monocoque Fuselage, Theoretical Analysis

By

M. FINE, B.A. and D. WILLIAMS, D.Sc. A.M.I.MECH.E.

LONDON: HIS MAJESTY'S STATIONERY OFFICE
Price 5*s.* 0*d.* net

Stress Concentration Due to Four-point Fixing at Front End of Monocoque Fuselage, Theoretical Analysis

By
M. FINE, B.A. and D. WILLIAMS, D.Sc., A.M.I.MECH.E.

COMMUNICATED BY THE DIRECTOR-GENERAL OF SCIENTIFIC RESEARCH (A), MINISTRY OF SUPPLY

Reports and Memoranda No. 2100
April, 1941*

Summary.—Introductory (Purpose of Investigation).—This report is a sequel to previous work by Williams, Starkey and Taylor (R. & M. 2098[1]) and by Williams and Fine (R. & M. 2099[2]) and treats the problem of the stress distribution in a stringer-reinforced cylindrical shell (representing a modern monocoque fuselage) under transverse loads when the reactions at the supported end are provided by four fixing points. It is assumed that these reactions are transmitted to the shell through four heavy longitudinal members, or longerons, and the purpose of the report is to discuss the manner in which the load in these members is passed on *via* the skin to the adjacent stringers.

Range of Investigation.—Two cases are considered. In the first the longerons are assumed to be of constant cross-section and to extend from end at end of the shell. In the second the longerons are tapered from the root outwards in such a way as to maintain a constant stress. Appendices I and III of the report treat the problems with some rigour and the solutions obtained are made the bases of quick approximate methods that can be applied with facility to any practical case.

The results obtained by the approximate methods agree very satisfactorily with those derived by the far longer basic method.

Conclusions.—From working out typical cases it is inferred that for the end-to-end constant-section longerons the disturbance due to the four-point fixing does not extend a greater distance from the root fixing than $\frac{1}{2}$ to $\frac{3}{4}$ of the average root diameter, this distance being greater the greater the value of the ratio of total stringer area to total skin area in the cross-section. It is found that the constant-stress longeron tapers very quickly and appears to offer a good practical basis for design. The most important stress concentration in both cases is the shear stress in the skin immediately adjacent to the longerons at their root ends, and reinforcement of the skin thickness in this region is probably essential in all practical cases, especially for the constant stress longeron. The extent of this stress concentration is indicated by certain contour diagrams of stress distribution included in this report.

CONTENTS

		Page
1.	Introduction	1
2.	The Circular Cylindrical Shell, Stringer Reinforced and Held at the Root at Four Points; Longeron Section Constant from Root to Tip	2
3.	Discussion of Results	3
4.	Stub Longerons	4
5.	Constant-stress Longeron	5
6.	Approximate Methods	5
7.	Some Test Results	10
8.	Conclusions	11
	References	12
Appendix I.	Detailed Method of Solution for Constant-section Longerons and Circular Section	12
Appendix II.	Method of Plotting Shear Stress Curves	20
Appendix III.	Solution for Constant-stress Longerons and Circular Section	20

1. *Introduction.*—Williams, Starkey and Taylor (R. & M. 2098[1]) investigated the stress distribution in a stringer-reinforced flat sheet representing the stressed-skin cover of a two spar monoplane wing. Williams and Fine (R. & M. 2099[2]), which is a sequel to the above, extended the investigation to the case of a box-beam with a cambered instead of a flat surface. It also

* R.A.E. Report No. A.D. 3144, received 29th April, 1941.

treated the tubular or shell-beam with circular, oval and trapezoidal cross-sections intended to represent various shapes of fuselage cross-section. In the first report the effect of connecting only the spar flanges at the root was found, but in the second report the assumption was made throughout that the stringers were all securely fastened at the fixed end. The present report deals with the stress distribution consequent upon fixing the root section at isolated points, and is therefore an extension of the latter investigation. The general scheme of the report and an account of the ground covered may conveniently be given here.

The first case considered is a cylindrical shell of circular cross-section uniformly reinforced by stringers and fitted with four longerons of constant cross-section symmetrically arranged. The method of solution for this case is outlined in the first section of the report and given fully in Appendix I. The results of two numerical examples worked by this method are next given and their implications discussed.

In practice it is seldom desirable for the longerons to extend from root to tip and in the case of fuselages use is often made of stub longerons. It is clear that if these are to be efficient they should be tapered in some way, preferably so as to ensure constant stress at all sections. A method of solving this problem of the constant-stress longeron is set out fully in Appendix III, still using a circular cross-section. The results obtained by applying this method to one of the numerical examples above mentioned are discussed and it is shown that, apart from a greater degree of shear stress concentration in the root panels adjoining the longerons than in the case of the uniform longerons previously considered, this type of design has practical merits.

The drawback to the methods of solution above alluded to is that they are rather lengthy. Approximate methods have therefore been devised to give much the same results far more quickly. These approximate methods are designed first to enable an oval section to be adequately represented by an " equivalent " circular section and then to provide a quick solution for the latter. The bases of the approximate methods are described and the formulae to be used are given. Curves are also shown which indicate how closely the approximate results approach those obtained by the more rigorous but longer methods.

To justify the method used for converting an oval section into an equivalent circular section it was necessary to solve the problem of the oval section shell by a suitable adaptation of the method of Appendix I. An actual fuselage section was taken and its outline closely represented by a combination of cycloids. The results of applying the rigorous method to this problem were then compared with those derived from the equivalent circular section, and, as the curves show, good agreement was obtained. The effort to represent an actual fuselage was made because a few results of tests on it were available and it was desired to compare these with the theoretical curves. Good agreement was not expected because the stub longerons used on this fuselage were short and of uniform section and therefore offer a problem not readily amenable to the present methods. There was however agreement on the order of the magnitude and distribution of the stresses. Some of the more important conclusions are set out in § 8.

2. *The Circular Cylindrical Shell, Stringer Reinforced and Held at the Root at Four Points; Longeron Section Constant from Root to Tip.*—

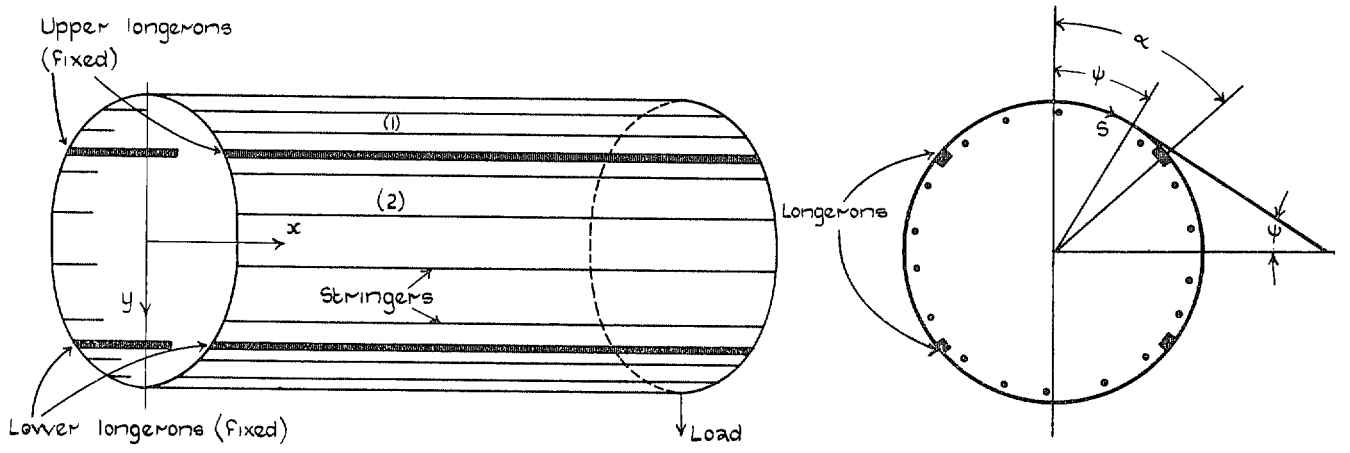

FIG. 1.

The general scheme of the analysis will be given first. We consider a circular cylindrical shell attached by four longerons to fixed points. The longerons are symmetrically placed about vertical and horizontal planes through the axis of the cylinder. The shell is uniformly reinforced by stringers which, for convenience, we replace by an equivalent sheet of thickness t_s capable of withstanding direct stress only. It is reinforced by transverse circular rings also. We assume the rings to be infinitely stiff in their own plane, so that all points on a ring move through the same vertical distance v under load, and perfectly flexible normal to their plane. We assume the rings are so close together that this is true for all sections.

The longitudinal displacement u in the representative quadrant shown above is considered separately for (*a*) surface 1, (*b*) surface 2 and (*c*) longeron. The vertical displacement v, normal to the axis of the tube, however, is assumed to be the same at all points of the periphery at any given section, *i.e.* it varies only with distance along the axis.

The longitudinal displacements in (*a*), (*b*) and (*c*) are written down in the form of three separate trigonometrical series with coefficients P_{1q}, P_{2q} (both of which are functions of ψ) and P_{aq} (constant coefficient) respectively that are later evaluated by applying those boundary conditions that are not inherently satisfied by the form of the series. A somewhat similar series with undetermined constant coefficients V_q is assumed for the vertical displacement v.

The condition of equilibrium in sheets 1 and 2, together with the condition of equality of displacement of these two sheets where they meet at the longeron, enable each of the coefficients P_{1q}, P_{2q} and P_{aq} to be expressed in terms of new constant coefficients A_q, V_q and V_0.

Finally the latter are evaluated by using the condition of equilibrium between sheets and longeron and the condition that at each section there must be equilibrium between the internal shear and the applied external load.

The method of solution is given in detail in Appendix I.

3. *Discussion of Results.*—

3.1. *Dimensions for Numerical Examples.*—The following dimensions were chosen for the two numerical examples that were worked:—

Thickness t of shear skin = 0·025 in.

Thickness t_s of stringer sheet (*i.e.* total stringer area divided by periphery) = 0·0144 in. (1st example), 0·0072 in. (2nd example)

Cross-sectional area of each longeron = 0·8 sq. in.

Length of shell = 240 in.

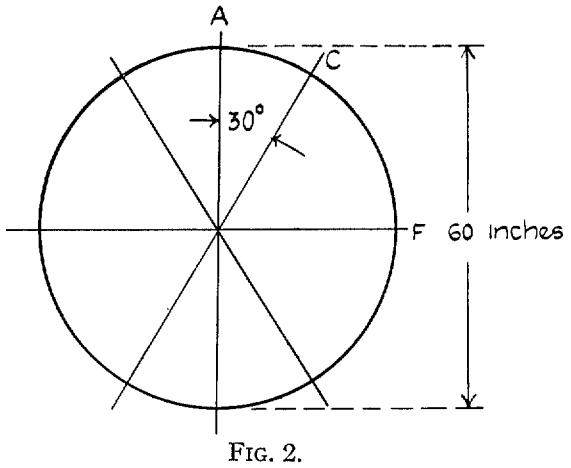

FIG. 2.

Ratio of Gt/Et_s (G and E being the elastic moduli) = 0·7 (1st example), 1·4 (2nd example).

Vertical load applied at free end and root fixed only at the four longerons.

3.2. *Direct Stress Distribution.*—We need only consider the quadrant AF (Fig. 2) in view of the symmetry of the structure. Fig. 3 shows the distribution of stress along the longeron C and along various stringers, two of them located in the arc AC and two in CF as shown in the inset diagram of Fig. 3. In each case the comparable stress distribution given by the simple engineering theory of beams is also plotted.

It will be noted that engineering theory is adequate except over a region extending from the root outwards to a distance equal to $\frac{3}{4}$ of the diameter. As the root is approached from the section defined by that distance, the stringer stresses maintain a constant value for another

$\frac{1}{4}$ diameter and only dip down to zero over the final $\frac{1}{2}$ diameter. Correspondingly the longeron stresses sweep up to their root value in the same distance. As the root value for the longeron stress is known, the curve of stress for the root region can almost be drawn in by eye since it has to be tangential to the engineering stress curve at $\frac{3}{4}$ diameter from the root. Especially is this possible after inspection of a typical curve such as that of Fig. 3.

3.3. *Effect of Altering the Ratio Gt/Et_s.*—The effect of changing the ration of shear to longitudinal stiffness Gt/Et_s is shown in Fig. 4, where t_s has been halved and the value of the ratio therefore doubled. No appreciable departure from engineering theory now takes place until a point is reached $\frac{2}{3}$ diameter from the root. Moreover, the downward dip of the stringer stress to zero and the corresponding up sweep of the longeron stress to its root value begins in earnest only $\frac{1}{4}$ diameter from the root as compared with $\frac{1}{2}$ diameter for the smaller stiffness ratio. A still thicker skin or smaller stringers would of course result in a further localisation of the region of serious departure from engineering theory.

3.4. *Shear Stress Distribution.*—Fig. 5 shows the distribution of shear stress for the lower value of the stiffness ratio just discussed. The region of serious departure from engineering theory is seen to be much the same as the corresponding region for the direct stresses. The amount of the departure from the simple theory is, however, of much greater importance, the maximum stress being many times greater than that given by that theory.

Considering the root section (Fig. 5) it is noted that over the arc AC, as was to be expected, the shear stress is of opposite sign to that given by engineering theory but that from C to F it has the same sign. We note also that, although the arc AC subtends only half the angle of the arc CF, the higher stringer stresses in AC make the maximum shear stress greater than the maximum in arc CF. These maxima are located immediately to the left and right of the longeron for infinitely close pitched stringers, but for a 6-in. pitch the stress at 3 in. from the longeron represents well enough the average stress in the panel. At the root this average has values above and below the longeron of about 5 and 4 times respectively that of the maximum shear stress given by engineering theory. The analysis of § 9 neglects the effects of finite frame flexibility lengthwise, of peripheral movements due to finite stiffness of the frames in their plane, and of relative movements at riveted joints. These effects will tend to reduce the shear stress and so this estimate is conservative. Fig. 6 shows the shear stress distribution in a different way and includes a contour diagram of stress that clearly indicates the regions of high stress. The very local character of these high stresses suggests that they can be reduced to predetermined limits by a correspondingly local reinforcement of the skin thickness. Such a thickening of the skin, increasing as it does the value of the ratio Gt/Et_s, will have the effect of reducing the stress rather more than inversely proportional to the skin thickness.

Figs. 7 and 8 show the corresponding stress diagrams when t_s is halved (ratio Gt/Et_s doubled). The effect of this change, as in the case of the direct stresses, is to localise the region of departure from engineering theory still further as well as to reduce the absolute value of the maximum shear stresses.

4. *Stub Longerons.*—In practical fuselage design it is seldom desirable to extend the longerons from end to end and, as their main function is to concentrate at four points at the root the loads that would otherwise be distributed among the stringers, the tendency is to cut them short at a point where their function has been largely carried out. It is obvious that if these stub longerons are constant in section they cannot be very efficient, for the stress at their outer end must be very small compared with that at the fixed end. Constant-section stub longerons have also the disadvantage that they induce a considerable degree of shear stress concentration at their outer as well as at their root ends. It is also clear that the root shear stresses must be greater for the stub longeron than for the continuous longeron of equal section, because the root longeron load, which is constant, must be got rid of in a shorter distance. It would therefore seem desirable to give the longerons some sort of taper.

5. *Constant-stress Longeron.*—The longeron will itself be most efficient when its stress is constant and equal to the maximum permissible stress. As the cross-sectional area of the stringers is usually constant from end to end, it is impossible to ensure constant stress in the longeron by giving it a longitudinal variation of sectional area, without stipulating negative values near the free end. In practice, however, we are concerned in ensuring a constant stress only in the root portion of the longeron and the variation of section thus obtained is little affected by an incorrect variation at points further away. The actual taper would not be carried further than a point somewhat short of the section where the area is reduced to that of a stringer.

Fortunately the problem of the constant-stress longeron does not offer much mathematical difficulty (R. & M. 1780[3]) and the analysis is given in Appendix III. The first numerical example of § 3.1 was worked out with the uniform longerons replaced by constant-stress longerons. The results are shown in Figs. 10 and 11. Fig. 10 gives the rate of taper and Fig. 11 shows the shear stress distribution at the longeron near the root. On comparing these with those for the uniform longeron shown in Fig. 5, it is seen that the shear stresses associated with the constant-stress longerons are, as expected, somewhat greater. It would be more useful, however, to compare the constant-stress tapered longeron with the uniform stub longeron which it is designed to replace. Not knowing the values of the stresses for the latter, one can only say that the tapered longeron scores distinctly in the matter of weight and that there is no reason to suppose that it compares unfavourably in the matter of the shear stresses induced.

A longeron that is properly tapered to give constant stress under a vertical transverse end load will in general not have a constant stress under a side transverse load. The root stress under the side load can of course be immediately found and a convenient way of determining whether the stress at any other point rises above the constant stress σ_v for the vertical load is as follows. It is clear that if the longeron root stress under side load is, say, r times σ_v (where r must be less than unity unless σ_v is below the allowable stress) the root sectional area could be reduced in the ratio r. Assuming this to be the new root section for the side load case, the proper taper for a constant stress can be found. If the curve of sectional area so found never rises above that of the actual taper, it may reasonably be assumed that the allowable longeron stress is never exceeded and that the shear stresses in the adjacent panels are not greater than those produced by the vertical load.

6. *Approximate Methods.*—It is rather a lengthy task to apply the above methods to numerical examples and it is therefore highly desirable from a design point of view to develop some approximate procedure which, while giving substantially the same results, can be applied far more quickly. Such an approximate procedure has been devised which can be applied with slight differences to both the constant-section and the constant-stress longeron. The required formulae are set out in the following sections, and curves are also given which show how nearly the results obtained approach those obtained by the longer method. These formulae apply to a shell of circular cross-section but it has been found that an oval section can be simply dealt with by converting it into an " equivalent " circular section before applying the formulae. Curves are given to show that the conversion method is accurate enough for practical purposes (*see* Fig. 12).

As the taper given to fuselages is usually small, and as also the effect considered here is a local one, the cross-section at the root may be justifiably assumed to apply at all points along the length. It is safe to do this because Reissner[4] has recently shown that the effect of taper is generally to reduce stress concentrations due to shear lag.

6.1. *Formulae for Circular Cross-sections with Constant-section Continuous Longerons.*—The formulae in §§ 6.1–6.3 are obtained by methods explained in § 6.4.

6.11. *Longeron stresses.*—The difference between longeron stress according to engineering theory (with longeron and stringers all fixed at the root) and the approximate longeron stress is d times the former stress, where d is given by the formula

$$d = (1/R)\ (1 - R)\ e^{-kx}, \qquad \ldots\ \ldots\ \ldots\ \ldots\ \ldots\ \ldots\ \ldots \quad (1)$$

where R = ratio of the second moment of the longerons about the neutral plane, to the second moment of the longerons and stringers combined,

i.e. $$1/R = 1 + \pi a t_s/4S\cos^2\alpha\,, \quad .. \quad .. \quad .. \quad .. \quad .. \quad .. \quad (2)$$

$$k = 2/lK^*\,, \quad .. \quad .. \quad .. \quad .. \quad .. \quad .. \quad .. \quad .. \quad (3)$$

where $$K = 1 - \frac{8}{\pi^2 R}\sum_n \frac{1}{n^2\left(\frac{1}{1+n^2\lambda^2} + \frac{n\pi\lambda\sinh n\lambda\,(\pi/2-\alpha)\cosh n\lambda\alpha}{4\cos^2\alpha\cosh n\lambda\pi/2} + \frac{\pi a t_s}{4S\cos^2\alpha}\right)}\,, \quad (4)$$

where n takes odd positive values. (λ is defined in eqn. (7) of § 9 : other symbols are defined at the beginning of § 9.)

This series is rapidly convergent and the curves of Fig. 12 are based on three terms of the series. The curves of Fig. 13 are drawn up, from eqns. (3) and (4), to obviate calculating series (4) and to give k rapidly.

6.12. *Shear stresses adjacent to longeron.*—The *excess* of the shear stress as calculated by the approximate method over that given by engineering theory gives, when divided by the latter stress,

$$\tau_1 = -lke^{-kx} \quad \text{on the crown side of the longeron} \quad .. \quad .. \quad .. \quad (5)$$

and $$\tau_2 = \frac{lk}{R}\,\frac{(1 - R - R\,\frac{at_s}{S}\tan\alpha)}{(1 + \frac{at_s}{S}\tan\alpha)}\,.e^{-kx} \quad \text{on the neutral axis side of the longeron.} \quad .. \quad .. \quad (6)$$

6.2. *Formulae for Circular Section with Constant-stress Longerons.*—6.21. *Taper of longeron cross-sectional area.*—The approximate longeron area S is given by the equation

$$S = S_0\left(1 - \frac{x}{l}\right) - \frac{\pi a t_s}{4\cos^2\alpha}(1 - e^{-k'x}) \text{ for } 0 \leqslant x \leqslant \frac{l}{2}\,, \quad .. \quad .. \quad (7)$$

(for $\frac{l}{2} \leqslant x \leqslant l$ we must replace x by $(l - x)$ in the exponent),

where $$k' = 2/lK_1 \quad .. \quad .. \quad .. \quad .. \quad .. \quad .. \quad .. \quad .. \quad (8)$$

and $$K_1 = 1 - \frac{8}{\pi^2}\sum_n \frac{1}{n^2\left\{\frac{1}{1+n^2\lambda^2} + \frac{n\pi\lambda\sinh n\lambda\,(\pi/2-\alpha)\cosh n\lambda\alpha}{4\cos^2\alpha\cosh n\lambda\pi/2}\right\}}\,, \quad (9)$$

n taking odd positive values. Fig. 13 again obviates the use of a long calculation in finding k'.

In practice of course the taper will not be carried beyond a point where the cross-section approaches that of a single stringer.

This series is similar to that for K given by eqn. (4) and is rapidly convergent. Five terms of the series give a longeron area which differs by a negligible amount from that of Fig. 10.

6.22. *Shear stresses adjacent to longeron.*—τ_1', τ_2' are the approximate shear stresses on the crown and neutral axis sides of the longeron respectively due to unit transverse load at the free end.

---

* It can be shown by St. Venant's principle, that the product lK approaches asymptotically a constant value as l is progressively increased, and that once l exceeds about twice the diameter, the root stress distribution changes little with further increase of l.

Then
$$\tau_1' = -\frac{t_s k' l L}{\pi t S_0 \cos^2\alpha} e^{-k'x}, \quad \ldots \quad (10)$$

$$\tau_2' = \frac{1}{4at\cos\alpha} + \frac{(\pi^2 - 16L\cos\alpha)\, t_s k' l}{16\pi t S_0 \cos^3\alpha} e^{-k'x}, \quad \ldots \quad (11)$$

where
$$L = \sum_n \frac{(-1)^{\frac{n-1}{2}} \left\{ \frac{\sin\alpha}{1+n^2\lambda^2} + \frac{\pi \sinh n\lambda(\pi/2-\alpha)\sinh n\lambda\alpha}{4\cos\alpha\cosh n\lambda\pi/2} \right\}}{n\left\{ \frac{1}{1+n^2\lambda^2} + \frac{\pi n\lambda \sinh n\lambda(\pi/2-\alpha)\cosh n\lambda\alpha}{4\cos^2\alpha\cosh n\lambda\pi/2} \right\}}, \quad \ldots \quad (12)$$

n taking odd positive values.

It is sufficiently accurate, for metal fuselages, to take

$$L = \frac{\pi}{4}\sin\alpha. \quad \ldots \quad (13)$$

6.3. *Shells of Oval Section.**—An oval section shell may conveniently be dealt with by first converting it into an " equivalent " circular section.

The dashed symbols refer to the equivalent circular section and the following additional notation is used (*see* Fig. 18) :—

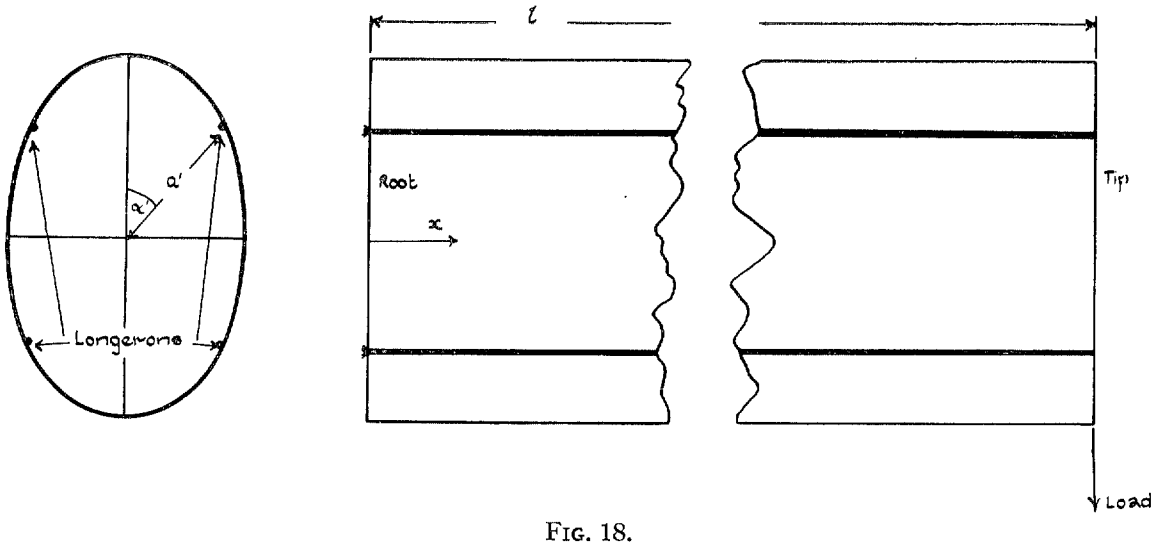

FIG. 18.

I = section moment of inertia—entire section

I_0 = section moment of inertia neglecting longerons

q_{ea} = shear stress adjacent to longerons on crown side
q_{eb} = shear stress adjacent to longerons on neutral axis side
} calculated for unit transverse load, by simple beam theory with entire root fixed.

q_a = shear stress corresponding to q_{ea}
q_b = shear stress corresponding to q_{eb}
} allowing for stress concentration.

* The authors are grateful to Mr. Rao for pointing out a mistake in the conversion, as originally stated, and for his help in correcting it.

6.31. *Basis of method of conversion.*—The following quantities, at any distance from the root, are made the same for the oval section and the equivalent circular section :—

(*a*) stresses in the longeron away from the root,
(*b*) loads in the longeron away from the root,
(*c*) shear stresses in the skin adjacent to the longeron away from the root,
(*d*) shear loads in the skin adjacent to the longeron away from the root,
(*e*) root stress in the longeron,
(*f*) root load in the longeron,
(*g*) strains corresponding to the above stresses.

There is thus agreement away from the root and at the root as regards the two shells. It is to be expected that there is agreement over the root region also. The method assumes this and comparison of the " conversion " method with more rigorous analysis verifies this for a particular case (Figs. 12 (*c*), 12 (*c'*)).

6.32. *Application of method.*—The above conditions become

$$\left.\begin{aligned} \alpha' &= \tfrac{1}{2}\sin^{-1}(2\pi I a t q_{ea}\cos\alpha/I_0),\\ a' &= a\cos\alpha\sec\alpha',\\ t_s' &= I_0/\pi a'^3,\\ t' &= t,\\ S' &= S. \end{aligned}\right\} \quad \ldots\ \ldots\ \ldots\ \ldots\ \ldots\ \ldots \quad (14)$$

Knowing the equivalent circular section from eqn. (14), the values of k and of k' corresponding to constant-area and constant-stress longeron respectively may be calculated.

The stresses are then given by eqns. (1), (5), (6), (10), (11), (13) as before and the taper to maintain constant stress by eqn. (7), provided that α, a and t_s in these formulae are replaced by α', a' and t_s' respectively.

There is one point to be noted in calculating α'. If α' is a solution of the first equation of (14), then (90 deg.— α') is also a solution; thus if $\alpha' = \frac{1}{2}\sin^{-1} 0{\cdot}5$, then $\alpha' = \frac{1}{2}\times 30$ deg. or $\frac{1}{2}\times 150$ deg. = 15 deg. or 75 deg.

A rule for deciding which value to take is obtained by actually evaluating α' against α for slightly oval shells and by using the knowledge that a circular shell must have itself as its equivalent. The analysis, which is not given here, leads to the following rule :— if the load is applied parallel to the major axis, take the value of α' which is greater than α and if both values of α' are greater than α choose the smaller ; if, however, the load is applied parallel to the minor axis, take the value of α' which is less than α and if both values of α' are less than α choose the greater.

6.4. *Basis of Approximate Method.*—6.41. *Constant-section longeron.*—The method is based on assuming d to be of the form given by eqn. (1). This gives d the correct value at $x = 0$. k is then determined by the condition that $\int_0^l d\,dx$ is to have the same value as that given by the more elaborate method, which we intend to short circuit. We thus obtain eqns. (3) and (4).

The shear stresses are obtained by assuming that τ_1/τ_2 is constant, that $\int_0^l \tau_1\,dx$ has the same value as that given by the more elaborate method and that the approximate longeron load is in equilibrium with the approximate adjacent shears. (These conditions automatically make $\int_0^l \tau_2\,dx$ also agree with the value given by the longer method.) Eqns. (5) and (6) follow from these conditions.

6.42. *Constant-stress longeron.*—The " constant-stress " solution shows that the variation of the longeron cross-sectional area can best be represented by a linear taper from root to tip, upon which is superimposed a further reduction of area that is independent of the longeron root section and that is also practically constant over most of the length. The dip down to zero value at the ends takes place over a restricted length the extent of which depends upon the size of the cross-section. Fig. 19 shows what is meant.

OA represents the root cross-sectional area of the constant-stress longeron, its value being fixed by the allowable stress. To get the proper variation of the cross-section we first represent a linear taper to zero by the straight line AB, and then draw a parallel line A_1B_1 where AA_1 is independent of the size of the root section of the longeron and depends only on the position of the longeron (given by α), the stringer-sheet thickness t_s and the radius a of the fuselage cross-section. Its value δ_0 is given by

$$\delta_0 = \pi a t_s / 4 \cos^2 \alpha.$$

This value of δ_0 is the correct value for a long cylinder and is a very good approximation for a fuselage. It is now necessary to " join " the two straight lines by curves CA and C_1B. These are symmetrical in the sense that intercepts EE_1 and FF_1, equidistant from the central ordinate PP_1, are equal. The true curve "joining" the two parallel lines through A and A_1 can be well represented by an exponential curve CA expressed in the form

$$\delta = \delta_0 e^{-k'x},$$

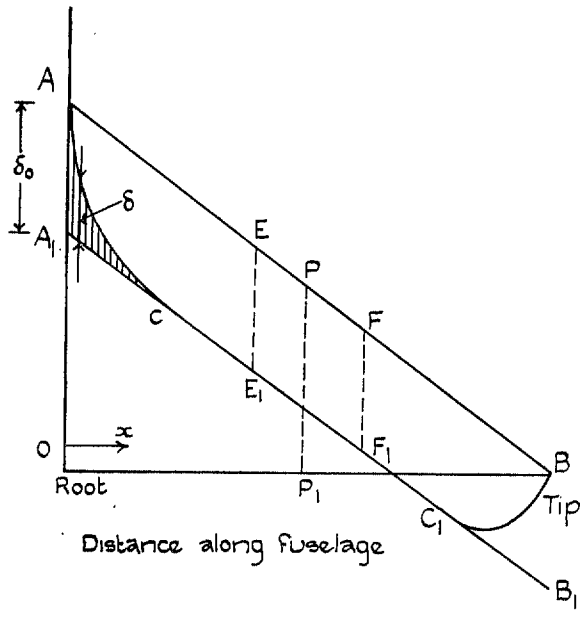

FIG. 19.

where the exponent k' is such as to make the area intercepted between A_1C and AC (shown shaded) equal to the corresponding area intercepted by A_1C and the curve obtained by the more rigorous method.

The approximate shear stresses are determined by assuming that $\left(\tau_2' - \frac{1}{4\,at\cos\alpha}\right)/\tau_1'$ is constant, that the approximate longeron load is in equilibrium with the adjacent shear loads and by making $\int_0^l \tau_1'\,dx$ have the same value as by the longer method.

6.5. *Accuracy of Approximate Methods.*—The curves of Fig. 12 which are based on using only three terms of the series for K in eqn. (4), indicate that this approximate method, while being rapid, is sufficiently accurate for all practical purposes in the case of the circular shell with constant-section longerons and that the assumption made in converting non-circular to equivalent circular shells is valid.

In Fig. 12, curves (*a*) and (*a'*) show a comparison between the results obtained by the exact and the approximate methods for the first numerical example of § 3.1. Curves (*a*) give the direct stresses in the longeron and curves (*a'*) the corresponding shear stresses. Curves (*b*) and (*b'*) show the corresponding results for the second numerical example. Both these sets of curves apply to a shell of circular cross-section.

As explained above it is necessary in dealing with a shell of oval cross-section to find the equivalent circular cross-section before applying the approximate methods proper. It was desirable therefore first to work out the exact results for an oval cross-section by an adaptation (not included in this report) of the analytical solution of § 9. The shape of the oval chosen was

the fuselage cross-section of an actual fighter aeroplane and it was found possible to represent this very closely by a cycloid and its reflexion in the axis of symmetry joining two cusps. The results obtained are shown in Fig. 12 by the full curves of (*c*) and (*c'*). The approximate method was applied by first converting the oval section into the equivalent circular section in the way described in § 6.31 and then using this as a basis for computing the stresses. The results are shown in Fig. 12 (*c*) and (*c'*) where also the stresses given by the simple engineering theory (with all stringers fixed at the root section) are shown for comparison. It is seen that there is satisfactory agreement between the approximate and the " exact " methods.

The corresponding curves for the constant-stress tapered longeron are shown for a shell of circular cross-section in Figs. 10 and 11 where the results obtained by the approximate method are shown dotted. The curves obtained for rate of taper of the longerons by the exact and the approximate methods are indistinguishable (Fig. 10) and the shear stresses are also in good agreement (Fig. 11).

It is to be expected that the same good agreement would obtain between the results of the approximate and the " exact " methods for an oval-section shell with constant-stress longerons.

6.6. *Practical Application of Approximate Methods.*—6.61. *Constant-section longeron.*—In order to facilitate the application of the method the curves of Fig. 13 have been drawn. These curves enable the die-away factor k to be readily determined when the structural dimensions of the equivalent circular section are known.

The curves are used as follows :—First the value of the non-dimensional coefficient $\mu = at_s/S$ is calculated and the value of ka corresponding to this value of μ and the known value of α is read from the graph directly or by interpolation. This value of ka is then multiplied by $9\sqrt{\frac{Gt}{Et_s}}$ to give the final value of ka and hence of k.

It is to be noted that the value of k thus obtained is independent of the length of the shell the assumption having been made that the length is at least twice the diameter.

The stress in the longeron may now be obtained very simply by the use of eqns. (1) and (2) of § 6.11 above, in conjunction with the known stress given by the simple engineering theory. The shear stresses adjacent to the longeron (where they are greatest) are similarly obtained by the use of eqns. (5) and (6) of § 6.12 and the known stresses as given by simple engineering theory.

6.62. *Constant-stress longeron.*—The die-away factor k' may be obtained similarly from Fig. 13.

Thus, in order to find k' the value of $k'a$ corresponding to the known value of α is determined from the graph and this value is multiplied by $9\sqrt{\frac{Gt}{Et_s}}$ to give the final value of $k'a$ and hence of k'.

The longeron taper is now readily obtainable from eqns. (7) and (8) and the shear stresses are obtained from eqns. (10), (11) and (13).

In this case also the same assumption is made as was made in § 6.61, *viz.* the shell length is at least twice the diameter.

7. *Some Test Results.*—The particular fuselage mentioned in § 6.5 was one for which a few test results happened to be available and these are plotted in Figs. 14, 15, 16 and 17 for comparison with the results calculated by the present methods. The type of longeron used in this fuselage was a short stub member of constant section and the adjacent shear panels were reinforced by patch plates to withstand the expected concentration of shear stress. Thus the conditions were not satisfied for the application of either of the theoretical cases—constant-section or constant-stress longeron—dealt with in this report. It would be surprising therefore if the test results agreed well with either of the two methods. As however the conditions more nearly approach

those of the continuous constant-section longeron (at least close to the root), this is the case with which the test results have been compared. The theoretical results were worked out first, assuming that the skin contributed nothing to the effective stringer cross-sectional area (Figs. 14 and 15) and next assuming that it was completely effective (Figs. 16 and 17). By adopting the latter hypothesis we see from Fig. 16 that fair agreement between the curve and the test points is obtained over the root part of the stub longeron. Now the rate of die-away of the load in the stub longeron must clearly be higher than that in a longeron extending from end to end of the fuselage, for the load must drop almost to zero in the short length of the stub longeron. The way we have obtained the agreement shown by Fig. 16 is by assuming an excessive amount (the whole in fact) of the skin to be behaving as a stringer, for the greater the stringer area the greater the rate of die-away. If in actual fact the longeron had been continuous all the way, the rate of die-away would have been less and agreement between test and theory, both under these conditions, would presumably be obtained by assuming an appropriate fraction (less than the whole) of the skin to be added to the stringer area. It is likely that the opposite extreme assumption (Fig. 14) whereby the skin takes no end load makes the die-away too slow in all cases. The most suitable intermediate assumption is not known and the need for experimental work for settling points like these is clear. Failing this it is safest to assume that the skin carries no end load for the purpose of calculating the longeron stress and carries its full share when the shear stresses are being estimated.

8. *Conclusions.*—By generalising from the above examples, we are led to the following conclusions.

8.1. *Constant-section Longerons Continuing from End to End of Shell (or Fuselage).*—(i) For a stringer-reinforced cylindrical shell subject to a single transverse load at its free end and fixed at the root by four constant-section longerons that stretch from end to end of the shell the region where the stress appreciably departs from that given by the ordinary engineering theory of beams is confined to the root section and its immediate neighbourhood.

(ii) The greater the value of the ratio Gt/Et_s the more restricted is that region : with a value of 0·7 the region extends from the root outwards to a distance equal to $\frac{3}{4}$ diameter, but a value of 1·4 reduces the distance to $\frac{1}{2}$ diameter. It is of interest to note that, for " vertical " loading, the rate of decay is most rapid when the longerons are near the top and bottom of the fuselage ($\alpha = 20$ to 30 deg.).

(iii) The direct stress in the longerons and the shear stresses in the adjoining panels over this root region can be estimated accurately enough by making use of the approximate method, described in this report.

(iv) Large shear stresses are induced in the sheet immediately adjacent to the longeron at the root. The area of high shear stress, however, is very limited so that it should be an easy matter to reduce the stresses to any desired degree by increasing the skin thickness. The actual extent of these restricted areas of high shear stresses may be estimated by means of the approximate method in conjunction with the stress contours for typical cases given in Figs. 6 and 8.

8.2. *Constant-stress Tapered Longerons.*—In practical design it will usually be undesirable to carry the longerons from end to end, and therefore the correct taper to use for an abbreviated longeron becomes important, for the use of stub longerons of constant section is inefficient from the weight point of view. Based on the rigorous method given in Appendix III, an easily applied approximate method has therefore been included, (§ 6.2), which enables the correct taper for maintaining constant stress in the longeron to be found and which also gives the degree of shear stress concentration in the adjoining panels. In practice the taper should clearly not be carried beyond a point where the cross-sectional area of the longeron has dropped to that of a stringer, and would normally not be carried as far. The length of taper involved is of the order of one diameter. Over this length it may be convenient to taper the longeron in steps rather than continuously and so long as no fewer than three steps are used it is unlikely that the shear stresses will be appreciably increased thereby.

The shear stresses associated with the constant-stress longeron are somewhat higher than those for the constant-section longeron but probably very little, if at all, higher than for a constant-section stub longeron of the same length.

The effect of altering the ratio Gt/Et_s is much the same as that indicated in § 8.1 (ii) above.

8.3. *Effect on Flexural Stiffness of Four-point Root Fixing.*—A side issue, which has not been discussed in the body of the report, is the effect on the flexural stiffness of fixing a fuselage at only four points at the root section. The deflection can easily be deduced from the work of Appendix I and for the first example of § 3.1 the loss of stiffness was over 20 per cent. In estimating the flexural stiffness of a fuselage, therefore, a reduction of something like 20 per cent. should be allowed for, if the root section is held at only four points.

REFERENCES

No.	*Author*	*Title*
1	D. Williams, R. D. Starkey and R. H. Taylor	Distribution of Stress between Spar Flanges and Stringers for a Wing under Distributed Loading. R. & M. 2098, June, 1939.
2	D. Williams and M. Fine	Stress Distribution in Reinforced Flat Sheet, Cylindrical Shells and Cambered Box-beams under Bending Actions. R. & M. 2099, September, 1940.
3	H. L. Cox, H. E. Smith and C. G. Conway ..	Diffusion of Concentrated Loads into Monocoque Structures. R. & M. 1780, April, 1937.
4	E. Reissner	The Influence of Taper on the Efficiency of Wide Flanged Box-beams. *Journal Aer. Soc.* June, 1940.

APPENDIX I

Detailed Method of Solution for a Circular Shell with Constant-section Longerons

Definition of Terms Used.—Referring to Fig. 1 (p. 2), let the symbols be :—

- t thickness of metal sheet cover capable of withstanding shear stress only
- l length of shell
- a radius of cross-section
- S cross-sectional area of longeron
- O origin of co-ordinates at centre of root section
- x axial distance from O, positive towards free end
- y vertical distance from O, positive downwards
- u displacement in x-direction
- v displacement in y-direction
- s distance along the arc of a section measured clockwise from the crown of the section
- ψ $= s/a$
- α value of ψ at longeron
- W value of end transverse load
- σ tensile stress
- τ shear stress.

The surface between the crown and longeron is surface (1). The surface between the longeron and the neutral plane is surface (2). Suffices 1 and 2 refer to surfaces (1) and (2) respectively. A suffix α refers to the longeron at $\psi = \alpha$. When the meaning is plain the suffices will be omitted

Internal Equilibrium.—For the internal equilibrium of surfaces (1) and (2)

$$t_s \frac{\partial \sigma}{\partial x} + t \frac{\partial \tau}{\partial s} = 0 ,$$

but as $$\sigma = E \frac{\partial u}{\partial x}, \text{ and } \frac{\tau}{G} = \frac{\partial u}{\partial s} + \frac{dv}{dx} \sin \psi = \frac{\partial u}{a \partial \psi} + \frac{dv}{dx} \sin \psi,$$

we have, by substitution

$$E t_s \frac{\partial^2 u}{\partial x^2} + \frac{Gt}{a^2} \frac{\partial^2 u}{\partial \psi^2} + \frac{Gt}{a} \frac{dv}{dx} \cos \psi = 0 ,$$

or $$\frac{\partial^2 u}{\partial \psi^2} + a \frac{dv}{dx} \cos \psi + \frac{a^2 E t_s}{Gt} \frac{\partial^2 u}{\partial x^2} = 0 . \quad .. \quad .. \quad .. \quad .. \text{ (A.I.1)}$$

This is our fundamental differential equation for the displacements u and v, and is the same equation as previously derived in R. & M. 2099[2].

Assumed Forms of the Displacements.—We cannot assume that $u = \sum_q A_q \sin \frac{q\pi}{2} \frac{x}{l}$ ($q = 1, 3, 5,$ *etc.*) as was done in the previous investigations, for this makes u zero everywhere when $x = 0$. We therefore assume

$$\frac{\partial^2 u_r}{\partial x^2} \equiv \frac{1}{E} \frac{\partial \sigma_r}{\partial x} = P_{r0} + \sum_q P_{rq} \cos \frac{q\pi x}{l}, \ (r = 1, 2, \alpha) , \quad .. \quad .. \text{ (A.I.2)}$$

where q takes the values 1, 2, 3 . . . and the P's are functions of ψ but not of x. (By using a convergent series for the 2nd derivative, we ensure that the series for the 1st derivative and for the function u_r itself, obtained by successive integration, are also convergent.) We can allow for discontinuities by having different constants of integration for 1, 2 and α. Integrating eqn. (A.I.2) gives

$$\frac{\partial u_r}{\partial x} \equiv \frac{\sigma_r}{E} = \frac{\sigma_{r0}}{E} + x P_{r0} + \frac{l}{\pi} \sum_{q \geqslant 1} \frac{P_{rq}}{q} \sin \frac{q\pi x}{l}, \ (r = 1, 2, \alpha) , \quad .. \text{ (A.I.3)}$$

where σ_{r0} is the stress at $x = 0$.

But for surfaces (1) and (2), $\sigma_r = 0$ for $x = 0$ and $x = l$,

and so σ_{10}, P_{10}, σ_{20}, and P_{20} each vanish ; .. .. (A.I.3a)

and as $\sigma_a = 0$ when $x = l$,

$$\frac{du_a}{dx} = \frac{\sigma_{a0}}{E} \left(1 - \frac{x}{l} \right) + \frac{l}{\pi} \sum_{q \geqslant 1} \frac{P_{aq}}{q} \sin \frac{q\pi x}{l} , \quad .. \quad .. \quad .. \text{ (A.I.3b)}$$

σ_{a0} being the *known* longeron root stress.

Integrating eqn. (A.I.3) for surfaces (1) and (2) gives, using eqn. (A.I.3a),

$$u_r = u_{r0} + \frac{l^2}{\pi^2} \sum_{q \geqslant 1} \frac{P_{rq}}{q^2} \left(1 - \cos \frac{q\pi x}{l} \right), \ (r = 1, 2) , \quad .. \quad .. \text{ (A.I.4)}$$

where u_{r0} is the displacement at $x = 0$.

Integrating eqn. (A.I.3b) gives

$$u_a = \frac{l \sigma_{a0}}{2E} \left\{ 1 - \left(1 - \frac{x}{l} \right)^2 + \frac{l^2}{\pi^2} \sum_{q \geqslant 1} \frac{P_{aq}}{q^2} \left(1 - \cos \frac{q\pi x}{l} \right) \right\} , \quad .. \text{ (A.I.4a)}$$

the constant of integration being adjusted to make $u_a = 0$ when $x = 0$. We have now introduced three sets of unknown coefficients—P_{1q}, P_{2q} (both functions of ψ) and P_{aq} (constants)—and in addition two unknown functions of ψ—u_{10} and u_{20}—to express the longitudinal displacements u_1, u_2 and u_a.

For the vertical displacement v, we express dv/dx in the form

$$\frac{dv}{dx} = V_0 + \sum_{q \geqslant 1} V_q \cos \frac{q\pi x}{l}, \qquad \text{(A.I.5)}$$

where the V's are constant, since dv/dx is a function of x alone and therefore independent of ψ.

Solution of the Fundamental Differential Equation.—The quantity u as given by eqn. (A.I.4) and dv/dx as given by eqn. (A.I.5) must satisfy eqn. (A.I.1). Substituting from eqns. (A.I.4) and (A.I.5) in eqn. (A.I.1), equating terms independent of x, and remembering that u_{r0}, P_{rq} are functions of ψ, we have, for surfaces 1 and 2 respectively,

$$\frac{d^2u_{10}}{d\psi^2} + \frac{l^2}{\pi^2} \sum_{q \geqslant 1} \frac{d^2P_{1q}}{d\psi^2} \cdot \frac{1}{q^2} + aV_0 \cos \psi = 0, \qquad \text{(A.I.6a)}$$

$$\frac{d^2u_{20}}{d\psi^2} + \frac{l^2}{\pi^2} \sum_{q \geqslant 1} \frac{d^2P_{2q}}{d\psi^2} \cdot \frac{1}{q^2} + aV_0 \cos \psi = 0. \qquad \text{(A.I.6b)}$$

Equating coefficients of $\cos \frac{q\pi x}{l}$ gives, for surface 1,

$$-\frac{l^2}{\pi^2 q^2} \frac{d^2P_{1q}}{d\psi^2} + aV_q \cos \psi + P_{1q} \frac{a^2Et_s}{Gt} = 0,$$

or

$$\frac{l^2}{\pi^2} \frac{d^2P_{1q}}{d\psi^2} - \frac{q^2\pi^2}{l^2} \frac{a^2Et_s}{Gt} \cdot \frac{l^2}{\pi^2} P_{1q} = aq^2V_q \cos \psi,$$

which on putting

$$\frac{\pi^2a^2Et_s}{l^2Gt} = \lambda^2 \qquad \text{(A.I.7)}$$

gives

$$\frac{l^2}{\pi^2} \frac{d^2P_{1q}}{d\psi^2} - \lambda^2q^2 \frac{l^2}{\pi^2} P_{1q} = aq^2V_q \cos \psi. \qquad \text{(A.I.8a)}$$

Similarly for surface 2,

$$\frac{l^2}{\pi^2} \frac{d^2P_{2q}}{d\psi^2} - \lambda^2q^2 \frac{l^2}{\pi^2} P_{2q} = aq^2V_q \cos \psi. \qquad \text{(A.I.8b)}$$

The solutions of these two differential equations, which we shall discuss before considering eqns. (A.I.6a) and (A.I.6b) further, differ only in the arbitrary constants and may be written

$$\frac{l^2}{\pi^2} P_{rq} = B_{rq} \sinh q\lambda\psi + A_{rq} \cosh q\lambda\psi - \frac{aq^2V_q \cos \psi}{1 + q^2\lambda^2}, \qquad \text{A.I.(9)}$$

where $r = 1$ or 2 and B_{rq}, A_{rq} are constants.

As P_{1q} is even in ψ, $B_{1q} = 0$,

and

$$\frac{l^2}{\pi^2} P_{1q} = A_{1q} \cosh q\lambda\psi - \frac{aq^2V_q \cos \psi}{1 + q^2\lambda^2}. \qquad \text{(A.I.10a)}$$

Also as $P_{2q} = 0$ when $\psi = \pi/2$,

$$\frac{l^2}{\pi^2} P_{2q} = B_{2q} \sinh q\lambda\left(\frac{\pi}{2} - \psi\right) - \frac{aq^2V_q \cos \psi}{1 + q^2\lambda^2}. \qquad \text{(A.I.10b)}$$

But $P_{1q} = P_{2q}$ when $\psi = \alpha$, so that

$$\frac{l^2}{\pi^2} P_{2q} = A_{1q} \frac{\cosh q\lambda\alpha}{\sinh q\lambda\left(\frac{\pi}{2} - \alpha\right)} \sinh q\lambda\left(\frac{\pi}{2} - \psi\right) - \frac{aq^2 V_q \cos\psi}{1 + q^2\lambda^2} \quad \ldots \text{(A.I.11)}$$

and we may rewrite eqns. (A.I.10a) and (A.I.11), with a slight change of notation, in the form

$$\frac{l^2}{\pi^2} P_{1q} = A_q \sinh q\lambda\left(\frac{\pi}{2} - \alpha\right) \cosh q\lambda\psi - \frac{aq^2 V_q \cos\psi}{1 + q^2\lambda^2}, \quad \ldots \quad \ldots \text{(A.I.12a)}$$

$$\frac{l^2}{\pi^2} P_{2q} = A_q \cosh q\lambda\alpha \sinh q\lambda\left(\frac{\pi}{2} - \psi\right) - \frac{aq^2 V_q \cos\psi}{1 + q^2\lambda^2}. \quad \ldots \quad \ldots \text{(A.I.12b)}$$

The coefficients P, originally unknown functions of ψ, have thus been reduced to known functions of ψ and constant coefficients A_q and V_q.

We can now proceed to find the initial displacements u_{10} and u_{20}. Returning to eqns. (A.I.6a) and (A.I.6b), we find on substituting from eqn. (A.I.12a) in eqn. (A.I.6a) that

$$\frac{d^2 u_{10}}{d\psi^2} + \lambda^2 \sum_{q \geqslant 1} A_q \sinh q\lambda\left(\frac{\pi}{2} - \alpha\right) \cosh q\lambda\psi + \sum_{q \geqslant 0} \frac{aV_q \cos\psi}{1 + q^2\lambda^2} = 0,$$

which on integrating gives

$$u_{10} = -\sum_{q \geqslant 1} \frac{A_q}{q^2} \sinh q\lambda\left(\frac{\pi}{2} - \alpha\right) \cosh q\lambda\psi + \sum_{q \geqslant 0} \frac{aV_q \cos\psi}{1 + q^2\lambda^2} + B_1\psi + C_1,$$

but u_{10} is even in ψ so that $B_1 = 0$; and $u_{10} = 0$ when $\psi = \alpha$. This makes

$$u_{10} = \sum_{q \geqslant 1} \frac{A_q}{q^2} \sinh q\lambda\left(\frac{\pi}{2} - \alpha\right) (\cosh q\lambda\alpha - \cosh q\lambda\psi) + a(\cos\psi - \cos\alpha) \sum_{q \geqslant 0} \frac{V_q}{1 + q^2\lambda^2}. \quad \ldots \quad \ldots \quad \ldots \quad \ldots \text{(A.I.13a)}$$

Substituting similarly from eqn. (A.I.12b) in eqn (A.I.6b) we get

$$\frac{d^2 u_{20}}{d\psi^2} + \lambda^2 \sum_{q \geqslant 1} A_q \cosh q\lambda\alpha \sinh q\lambda\left(\frac{\pi}{2} - \psi\right) + a\cos\psi \sum_{q \geqslant 0} \frac{V_q}{1 + q^2\lambda^2} = 0.$$

Thus $$u_{20} = -\sum_{q \geqslant 1} \frac{A_q}{q^2} \cosh q\lambda\alpha \sinh q\lambda\left(\frac{\pi}{2} - \psi\right) + a\cos\psi \sum_{q \geqslant 0} \frac{V_q}{1 + q^2\lambda^2} + B_2\psi + C_2.$$

But $u_{20} = 0$ when $\psi = \frac{\pi}{2}$ and when $\psi = \alpha$, giving $C_2 = -\frac{\pi}{2} B_2$,

$$B_2 = \left\{ a\cos\alpha \sum_{q \geqslant 0} \frac{V_q}{1 + q^2\lambda^2} - \sum_{q \geqslant 1} \frac{A_q}{q^2} \cosh q\lambda\alpha \sinh q\lambda\left(\frac{\pi}{2} - \alpha\right) \right\} \Big/ \left(\frac{\pi}{2} - \alpha\right).$$

Thus $$u_{20} = \sum_{q \geqslant 1} \frac{A_q}{q^2} \cosh q\lambda\alpha \left\{ \frac{\left(\frac{\pi}{2} - \psi\right)}{\left(\frac{\pi}{2} - \alpha\right)} \sinh q\lambda\left(\frac{\pi}{2} - \alpha\right) - \sinh q\lambda\left(\frac{\pi}{2} - \psi\right) \right\}$$

$$+ a\left\{ \cos\psi - \frac{\left(\frac{\pi}{2} - \psi\right)}{\left(\frac{\pi}{2} - \alpha\right)} \cos\alpha \right\} \sum_{q \geqslant 0} \frac{V_q}{1 + q^2\lambda^2}. \quad \ldots \quad \ldots \text{A.I.(13b)}$$

The displacements u_r ($r = 1, 2$) are then given by eqn. (A.I.4) after substituting from eqns. (A.I.12a), (A.I.12b), (A.I.13a), (A.I.13b).

When $\psi = \alpha$, we have $u_1 = u_2$

$$= \sum_{q\geqslant 1}\left(1 - \cos\frac{q\pi x}{l}\right)\cdot\frac{1}{q^2}\cdot\left\{A_q \sinh q\lambda\left(\frac{\pi}{2} - \alpha\right)\cosh q\lambda\alpha - \frac{aq^2V_q\cos\alpha}{1+q^2\lambda^2}\right\}$$

$$- \sum_{q\geqslant 1}\frac{1}{q^2}\left\{A_q \sinh q\lambda\left(\frac{\pi}{2} - \alpha\right)\cosh q\lambda\alpha - \frac{aq^2V_q\cos\alpha}{1+q^2\lambda^2}\right\}$$

$$- \sum_{q\geqslant 1}\frac{\cos q\pi x/l}{q^2}\left\{A_q \sinh q\lambda\left(\frac{\pi}{2} - \alpha\right)\cosh q\lambda\alpha - \frac{aq^2V_q\cos\alpha}{1+q^2\lambda^2}\right\} \quad \text{..(A.I.14)}$$

and this must equal u_a as given by eqn. (A.I.4a), *viz.*

$$u_a = \frac{l\sigma_{a0}}{2E}\left(\frac{2x}{l} - \frac{x^2}{l^2}\right) + \frac{l^2}{\pi^2}\sum_{q\geqslant 1}\frac{P_{aq}}{q^2} - \frac{l^2}{\pi^2}\sum_{q\geqslant 1}\frac{P_{aq}}{q^2}\cos\frac{q\pi x}{l}. \quad \text{.. .. A.I.(15)}$$

It is now necessary that the right-hand side of eqns. (A.I.14) and (A.I.15) should be equal for all values of x and for the purpose of satisfying this condition we expand the expression $\frac{l\sigma_{a0}}{2E}\left(\frac{2x}{l} - \frac{x^2}{l^2}\right)$ in a Fourier series, thus :—

$$\frac{l\sigma_{a0}}{2E}\left(\frac{2x}{l} - \frac{x^2}{l^2}\right) = \frac{l\sigma_{a0}}{3E} - \frac{2l\sigma_{a0}}{E\pi^2}\sum_{q\geqslant 1}\frac{\cos q\pi x/l}{q^2}. \quad \text{.. .. .. (A.I.16)}$$

Substituting in eqn. (A.I.15) from eqn. (A.I.16) we have

$$u_a = \frac{l\sigma_{a0}}{3E} + \frac{l^2}{\pi^2}\sum_{q\geqslant 1}\frac{P_{aq}}{q^2} - \frac{l^2}{\pi^2}\sum_{q\geqslant 1}\frac{1}{q^2}\left(P_{aq} + \frac{2\sigma_{a0}}{lE}\right)\cos\frac{q\pi x}{l}\cdot \quad \text{..(A.I.17)}$$

It is to be remembered that up to this point the stress $E \cdot du_a/dx$ has been based on the assumption that the term $\frac{l\sigma_{a0}}{2E}\left(\frac{2x}{l} - \frac{x^2}{l^2}\right)$ is taken at its face value and not replaced by the first n terms of its Fourier Expansion. We must therefore look upon this expansion as merely a convenient method of obtaining the best possible values of P_{aq} in terms of A_q and V_q. Having obtained them we must, in testing the equality of eqns. (A.I.14) and (A.I.15), still retain the above term in its finite form.

Equating terms independent of x in eqns. (A.I.14) and (A.I.17) we obtain

$$\sum_{q\geqslant 1}\frac{1}{q^2}\left\{A_q \sinh q\lambda\left(\frac{\pi}{2} - \alpha\right)\cosh q\lambda\alpha - \frac{aq^2V_q\cos\alpha}{1+q^2\lambda^2}\right\} = \frac{l\sigma_{a0}}{3E} + \frac{l^2}{\pi^2}\sum_{q\geqslant 1}\frac{P_{aq}}{q^2}. \quad \text{(A.I.18)}$$

Leaving this for a moment and going on to equate coefficients of $\cos q\pi x/l$ in eqns. (A.I.14) and (A.I.17), we obtain

$$\frac{1}{q^2}\left\{A_q \sinh q\lambda\left(\frac{\pi}{2} - \alpha\right)\cosh q\lambda\alpha - \frac{aq^2V_q\cos\alpha}{1+q^2\lambda^2}\right\} = \frac{l^2}{\pi^2}\cdot\frac{1}{q^2}\left(P_{aq} + \frac{2\sigma_{a0}}{lE}\right),$$

whence $$\frac{l^2}{\pi^2}P_{aq} = A_q \sinh q\lambda\left(\frac{\pi}{2} - \alpha\right)\cosh q\lambda\alpha - \frac{aq^2V_q\cos\alpha}{1+q^2\lambda^2} - \frac{2\sigma_{a0}}{lE}\cdot\frac{l^2}{\pi^2}\cdot \quad \text{.. (A.I.19}$$

It is seen that this would also satisfy eqn. (A.I.18) identically if the series were taken to infinit (because $\sum_{q\geqslant 1} 1/q^2 = \pi^2/6$) but in so far as only a finite number of terms are taken it will on approximately satisfy eqn. (A.I.18). Now, provided we can find the constant coefficients V_q, V_0, we can write down all the displacements and consequently all the stresses.

Evaluation of Displacement Coefficients.—Three relations connecting A_q, V_q and V_0 may now be obtained by equating the internal to the external overall shear and by expressing the condition of equilibrium between the rate of change of the load in the longeron and the shears in the adjacent panels.

The shear across any section and the applied shear must be equal, *i.e.*

$$aGt\left[\int_0^{\alpha}\left(\frac{\partial u_1}{a\partial\psi}+\frac{dv}{dx}\sin\psi\right)+\int_{\alpha}^{\pi/2}\left(\frac{\partial u_2}{a\partial\psi}+\frac{dv}{dx}\sin\psi\right)\right]\sin\psi\,d\psi=\frac{W}{4}.$$

(If the load is not a single end load, then we express the shear in the form $W_0+\sum_{q\geqslant 1} W_q\cos\frac{q\pi x}{l}$).

On substituting in this equation for u_1, u_2, dv/dx in terms of their series form and equating terms independent of x we get

$$\int_0^{\alpha}\left\{V_0\sin\psi-\sum_{q\geqslant 1}\frac{\lambda A_q}{aq}\sinh q\lambda\left(\frac{\pi}{2}-\alpha\right)\sinh q\lambda\psi-\sin\psi\sum_{q\geqslant 0}\frac{V_q}{1+q^2\lambda^2}\right.$$

$$\left.+\sum_{q\geqslant 1}\frac{\lambda A_q}{aq}\sinh q\lambda\left(\frac{\pi}{2}-\alpha\right)\sinh q\lambda\psi+\sin\psi\sum_{q\geqslant 1}\frac{V_q}{1+q^2\lambda^2}\right\}\sin\psi\,d\psi$$

$$+\int_{\alpha}^{\pi/2}\left\{V_0\sin\psi-\sum_{q\geqslant 1}\frac{A_q}{aq^2}\frac{\sinh q\lambda\,(\pi/2-\alpha)\cosh q\lambda\alpha}{(\pi/2-\alpha)}\right.$$

$$\left.-V_0\sin\psi+\frac{\cos\alpha}{\pi/2-\alpha}\sum_{q\geqslant 0}\frac{V_q}{1+q^2\lambda^2}\right\}\sin\psi\,d\psi=\frac{W}{4\,Gat},$$

which, on integration, becomes

$$\sum_{q\geqslant 1}\left\{\frac{V_q\cos\alpha}{1+q^2\lambda^2}-\frac{A_q}{aq^2}\sinh q\lambda\left(\frac{\pi}{2}-\alpha\right)\cosh q\lambda\alpha\right\}=\frac{W\,(\pi/2-\alpha)}{4\,Gat\cos\alpha}-V_0\cos\alpha. \quad \ldots \text{(A.I.20)}$$

This is the first of the relations mentioned at the beginning of § 1.4. It should be noted that the relation contains V_0 and all the coefficients A_q, V_q.

Equating coefficients of $\cos\frac{q\pi x}{l}$ then gives

$$-\int_0^{\alpha}\left\{\frac{\lambda A_q}{q}\sinh q\lambda\left(\frac{\pi}{2}-\alpha\right)\sinh q\lambda\psi+\frac{aV_q\sin\psi}{1+q^2\lambda^2}-aV_q\sin\psi\right\}\sin\psi d\psi$$

$$+\int_{\alpha}^{\pi/2}\left\{\frac{\lambda A_q}{q}\cosh q\lambda\alpha\cosh q\lambda\left(\frac{\pi}{2}-\psi\right)-\frac{aV_q\sin\psi}{1+q^2\lambda^2}+aV_q\sin\psi\right\}\sin\psi\,d\psi=0.$$

i.e.
$$\lambda aq^2\,V_q\frac{\pi}{4}+\frac{A_q}{q}\cos\alpha\cosh q\lambda\frac{\pi}{2}=0. \quad \ldots \text{(A.I.21)}$$

This is the second relation. It contains one A_q and the corresponding V_q and no other unknowns.

For equilibrium at the longeron ($\psi=\alpha$), we have

$$\left[\frac{d}{dx}(S\sigma_a)+t\,(\tau_2-\tau_1)\right]_{\psi=\alpha}=0,$$

or
$$\frac{d}{dx}\left(S\frac{du_a}{dx}\right)+\frac{Gt}{Ea}\left[\frac{\partial u_2}{\partial\psi}-\frac{\partial u_1}{\partial\psi}\right]_{\psi=\alpha}=0,$$

i.e.
$$\frac{dS}{dx}\frac{du_a}{dx}+S\frac{d^2u_a}{dx^2}+\frac{Gt}{Ea}\left[\frac{\partial u_2}{\partial\psi}-\frac{\partial u_1}{\partial\psi}\right]_{\psi=\alpha}=0. \quad \ldots \text{(A.I.22)}$$

If S is constant $S\frac{d^2u_a}{dx^2}$ is known as a cosine series. If S is not constant we must express the first two terms on the left-hand side of eqn. (A.I.22) as a cosine series in terms of the coefficients A_q, V_q, and σ_{a0} giving us

$$\frac{dS}{dx}\cdot\frac{du_a}{dx}+S\frac{d^2u_a}{dx^2}=K_0+\sum_{q\geqslant 1}K_q\cos\frac{q\pi x}{l}, \quad \ldots \quad \ldots \quad \ldots \text{(A.I.23)}$$

which reduces, if S is constant, to

$$K_0=-\frac{S\sigma_{a0}}{lE}, \quad K_q=SP_{aq}, \quad \ldots \quad \ldots \quad \ldots \quad \ldots \text{(A.I.24)}$$

where P_{aq} is given by eqn. (A.I.19). The remaining term of the left-hand side of eqn. (A.I.22)

$$\frac{Gt}{Ea}\left[\frac{\partial u_2}{\partial\psi}-\frac{\partial u_1}{\partial\psi}\right]_{\psi=\alpha}$$

$$=\frac{Gt}{Ea}\left[\frac{a\cos\alpha}{\pi/2-\alpha}\sum_{q\geqslant 0}\frac{V_q}{1+q^2\lambda^2}-\frac{1}{\pi/2-\alpha}\sum_{q\geqslant 1}\frac{A_q}{q^2}\sinh q\lambda\left(\frac{\pi}{2}-\alpha\right)\cosh q\lambda\alpha\right.$$

$$\left.+\sum_{q\geqslant 1}\frac{\lambda A_q}{q}\cosh q\frac{\lambda\pi}{2}\cos q\frac{\pi x}{l}\right]. \quad \ldots \quad \ldots \quad \ldots \quad \ldots \text{(A.I.25)}$$

Substituting from eqns. (A.I.25) and (A.I.23) in eqn. (A.I.22) and using eqn. (A.I.20) gives us, on equating terms independent of x,

$$K_0+\frac{Gt}{Ea}\cdot\frac{W}{4\,Gt\cos\alpha}=0,$$

i.e.

$$K_0+\frac{W}{4\,Ea\cos\alpha}=0. \quad \ldots \quad \ldots \quad \ldots \quad \ldots \text{(A.I.26)}$$

This is an incidental result that was known beforehand giving the load in the longeron at its root under the given bending moment. Equating coefficients of $\cos\frac{q\pi x}{l}$ gives the relation

$$K_q+\frac{Gt}{Ea}\frac{\lambda A_q}{q}\cosh q\lambda\frac{\pi}{2}=0. \quad \ldots \quad \ldots \quad \ldots \quad \ldots \text{A.I.(27)}$$

This is the third relation. When S is constant this relation contains one A_q and one V_q only. If S is not constant this equation contains all the A_q, V_q. Eqns. (A.I.27) and (A.I.21) suffice to determine A_q and V_q and then eqn. (A.I.20) gives V_0.

When S is constant the solution of these equations is

$$V_q=-\frac{2l\sigma_{a0}\sec\alpha}{\pi^2aq^2E}\Big/\left\{\frac{1}{1+q^2\lambda^2}+\frac{\lambda\,q\,\pi\sinh q\lambda\left(\frac{\pi}{2}-\alpha\right)\cosh q\lambda\alpha}{4\cos^2\alpha\cosh q\lambda\pi/2}+\frac{\pi at_s}{4S\cos^2\alpha}\right\}, \text{(A.I.28)}$$

$$A_q=-\frac{\lambda a\pi\sec\alpha\,q^3}{4\cosh q\lambda\pi/2}V_q, \quad \ldots \quad \ldots \quad \ldots \quad \ldots \quad \ldots \quad \ldots \text{(A.I.29)}$$

$$V_0=\frac{W(\pi/2-\alpha)\sec^2\alpha}{4Gat}+\frac{l\sigma_{a0}}{3aE\cos\alpha}+\frac{\pi at_s}{4S}\sec^2\alpha\sum_{q\geqslant 1}V_q. \quad \ldots \text{(A.I.30)}$$

When S varies with x the method of solution in general entails a prohibitive amount of labour. A notable exception is the longeron tapered to maintain constant stress.

Accuracy of Solution.—The stresses and displacements are thus obtained as infinite series. Taking only a finite number of terms will therefore give values which are not exact. Suppose we take n terms.

Then eqns. (A.I.3a), (A.I.4), (A.I.12a), (A.I.13a), (A.I.12b), (A.I.13b) give for the longitudinal displacements

$$u_a = \frac{l\sigma_{a0}}{2E}\left\{1 - \left(1 - \frac{x}{l}\right)^2\right\} + \frac{l^2}{\pi^2}\sum_{q=1}^{n}\frac{P_{aq}}{q^2}\left(1 - \cos\frac{q\pi x}{l}\right), \qquad \text{(A.I.31)}$$

where P_{aq} is given by eqn. (A.I.19),

$$u_1 = a\,(\cos\psi - \cos\alpha)\,V_0 + \sum_{q=1}^{n}\left\{\frac{A_q}{q^2}\sinh q\lambda\left(\frac{\pi}{2} - \alpha\right) - \frac{a\,(\cos\psi - \cos\alpha)\,V_q}{1 + q^2\lambda^2}\right\}\left(1 - \cos\frac{q\pi x}{l}\right), \qquad \text{(A.I.32a)}$$

$$u_2 = \frac{\pi/2 - \psi}{\pi/2 - \alpha}\sum_{q=1}^{n}\frac{A_q}{q^2}\sinh q\lambda\,(\pi/2 - \alpha)\cosh q\lambda\alpha + aV_0\cos\psi - a\left(\frac{\pi/2 - \psi}{\pi/2 - \alpha}\right)\cos\alpha\sum_{q=0}^{n}\frac{V_q}{1 + q^2\lambda^2} - \sum_{q=1}^{n}\left\{\frac{A_q}{q^2}\cosh q\lambda\alpha\sinh q\lambda\,(\pi/2 - \psi) - \frac{aV_q\cos\psi}{1 + q^2\lambda^2}\right\}\cos\frac{q\pi x}{l}. \qquad \text{(A.I.32b)}$$

From eqn. (A.I.5)

$$\frac{dv}{dx} = V_0 + \sum_{q=1}^{n} V_q\cos\frac{q\pi x}{l}, \qquad \text{(A.I.33)}$$

where, from eqn. (A.I.20),

$$V_0 = \frac{W\,(\pi/2 - \alpha)}{4G\,at\cos^2\alpha} - \sum_{q=1}^{n}\left\{\frac{V_q}{1 + q^2\lambda^2} - \frac{A_q}{aq^2}\sinh q\lambda\,(\pi/2 - \alpha)\cosh q\lambda\alpha\sec\alpha\right\}. \qquad \text{(A.I.34)}$$

Examination of the analysis shows that only one condition of the problem is not satisfied. The displacement of the longeron is not equal to the displacements of points on the adjacent sheets, although the displacements of the sheets are the same. Fig. 9 shows the displacements of the longeron and adjacent sheets given by twenty terms for a particular example. The agreement between the two displacements is quite good.

A clearer idea of the inaccuracy may be obtained as follows:—Beyond one diameter from the root the difference between the displacements is constant (and therefore the stresses are the same). If the longeron be uniformly compressed so as to bring it into coincidence with the sheets one diameter from the root, then the ratio of the required compressive stress to the longeron root stress is a measure of the error. Knowing the displacements this stress may be readily calculated. For the example considered it is less than 4 per cent. of the root stress.

When performing a calculation based on this report it will be necessary to take enough terms to ensure that the above error is reasonably small. A noteworthy feature of the method is that the terms are evaluated with the same ease for any number of terms.

APPENDIX II

Method of Plotting Shear Stress Curves

The series for the shear stresses obtained from eqns. (A.I.4), (A.I.12a), (A.I.12b), (A.I.13a) and (A.I.13b) do not converge very rapidly. The series obtained by term-by-term integration converge quite rapidly and the gradient of curves thus obtained gives the value of the shear stress at any point.

A simple example of this method is given here. Consider the series

$$\frac{3}{4} + \sum_q \frac{(-1)^{(q-1)/2} \cos q\pi x/l}{q\pi} = S,$$

where q is odd and greater than 0.

The sum of 6 terms gives very poor agreement with the sum to infinity especially at $x = 0$ and l. Integrating this series from l to x we obtain

$$-\int_l^x S dx = \frac{3}{4}(l - x) - l \sum_q \frac{(-1)^{\frac{q-1}{2}}}{q^2\pi^2} \cdot \sin \frac{q\pi x}{l} .$$

Therefore

$$-\frac{1}{l}\int_l^x S dx = \frac{3}{4}\left(1 - \frac{x}{l}\right) - \sum_q \frac{(-1)^{\frac{q-1}{2}}}{q^2\pi^2} \sin \frac{q\pi x}{l} .$$

The sum of 6 terms of the series agrees very well with the sum to infinity. In view of this, the curves of shear stresses given in this report have been obtained by measuring the slopes of the easily drawn curves obtained by analytically integrating the shear stress expressions. This example is rather extreme, for the curve obtained by integrating the series may be easily differentiated graphically as it consists of two straight lines. But even when the curvature changes, graphical differentiation of such an integrated series will give a more accurate value than the actual series, especially at the extreme values.

APPENDIX III

Constant-stress Longeron

Instead of eqn. (A.I.3a), we have, since $\sigma_a = \sigma_{a0}$ for all x,

$$du_a/dx = \sigma_{a_0}/E , \quad \ldots\ldots\ldots\ldots\ldots\ldots \text{(A.I.3a)'}$$

where a dash over the number of the equation indicates that it corresponds to the undashed equation in Appendix I.

Integrating this gives

$$u_a = \sigma_{a0} x/E , \ldots\ldots\ldots\ldots\ldots\ldots\ldots\ldots \text{(A.I.4a)'}$$

since $u_a = 0$ when $x = 0$.

From eqn. (A.I.14)

$$\left[u_1\right]_{y=a} = \sum_{q \geqslant 1} \frac{1}{q^2} \left\{ A_q \sinh q\lambda\left(\frac{\pi}{2} - \alpha\right) \cosh q\lambda\alpha - \frac{aq^2 V_q \cos \alpha}{1 + q^2\lambda^2} \right\}$$

$$- \sum_{q \geqslant 1} \frac{\cos q\pi x/l}{q^2} \left\{ A_q \sinh q\lambda\left(\frac{\pi}{2} - \alpha\right) \cosh q\lambda\alpha - \frac{aq^2 V_a \cos \alpha}{1 + q^2\lambda^2} \right\} \text{(A.I.14)'}$$

and this must equal u_a as given by eqn. (A.I.4a)'. For convenience we expand u_a in a Fourier series

$$u_a \equiv \sigma_{a0}x/E = l\sigma_{a0}/2E - \frac{\sigma_{a0}}{E} \cdot \frac{2l}{\pi^2} \sum_{q \geqslant 1} \frac{1-(-1)^q}{q^2} \cos \frac{q\pi x}{l} \quad \ldots \quad \ldots \quad \ldots \text{(A.I.17)'}$$

Equating terms independent of x in eqns. (A.I.17)' and (A.I.14)' gives

$$\sum_{q \geqslant 1} \frac{1}{q^2} \left\{ A_q \sinh q\lambda \left(\frac{\pi}{2} - \alpha \right) \cosh q\lambda\, \alpha - \frac{aq^2 V_q \cos \alpha}{1 + q^2\lambda^2} \right\} = \frac{l\sigma_{a0}}{2E} . \quad \ldots \text{(A.I.18)'}$$

Equating coefficients of $\cos q\pi x/l$ in eqns. (A.I.17)', (A.I.14)' gives

$$\frac{l^2}{\pi^2} \frac{2\sigma_{a0}}{lE} (1 - (-1)^q) = A_q \sinh q\lambda \left(\frac{\pi}{2} - \alpha \right) \cosh q\lambda\alpha - \frac{aq^2 V_q \cos \alpha}{1 + q^2\lambda^2} . \quad \ldots \text{(A.I.19)'}$$

If an infinite number of terms were taken then eqn. (A.I.18)' would be identically satisfied in virtue of eqn. (A.I.19)'. In so far as a finite number of terms is taken eqn. (A.I.18)' is only approximately satisfied.

The conditions expressing the equality of externally applied and internally produced shear are the same as before and are given by eqns. (A.I.20) and (A.I.21) which, with eqn. (A.I.19)' suffice to determine A_q, V_q, V_0 and hence the stresses everywhere.

To find the area of the longeron we express the condition for equilibrium.

We assume first that

$$\frac{dS}{dx} = S' + \sum S_q \cos \frac{q\pi x}{l} , \quad \ldots \quad \ldots \quad \ldots \quad \ldots \quad \ldots \quad \ldots \text{(A.III.1)}$$

giving

$$S = S_0 + S'x + \frac{l}{\pi} \sum \frac{S_q}{q} \sin q\pi x/l , \quad \ldots \quad \ldots \quad \ldots \quad \ldots \text{(A.III.2)}$$

where S_0 is the root area.

For equilibrium at the longeron

$$\left[\frac{d}{dx} (S\sigma_{a0}) + t(\tau_2 - \tau_1) \right]_{\psi=\alpha} = 0,$$

which gives

$$S'\sigma_{a0} + \sigma_{a0} \sum S_q \cos q\pi x/l + \frac{Gt}{a} \left[\frac{a \cos \alpha}{\frac{\pi}{2} - \alpha} \sum_{q \geqslant 0} \frac{V_q}{1 + q^2\lambda^2} \right.$$

$$\left. - \frac{1}{\frac{\pi}{2} - \alpha} \sum_{q \geqslant 1} \frac{A_q}{q^2} \sinh q\lambda \left(\frac{\pi}{2} - \alpha \right) \cosh q\lambda\alpha + \sum_{q \geqslant 1} \frac{\lambda A_q}{q} \cosh q\lambda\pi/2 \cos q\pi x/l \right] = 0 . \quad \ldots \text{(A.I.25)'}$$

On equating coefficients of terms independent of x in right-hand side and left-hand side of eqn. (A.I.25)′ and using eqn. (A.I.20) we get

$$S'\sigma_{a0} + \frac{W}{4a\cos\alpha} = 0\,;$$

but $$\sigma_{a0} = \frac{Wl}{4aS_0\cos\alpha}\,,$$

and therefore $S_0 = -lS'$ .. .. (A.III.3)

and this, with eqn. (A.III.2), gives $S = 0$ when $x = l$. Equating coefficients of $\cos q\pi x/l$ in eqn. (A.I.25)′ gives

$$S_q = -\frac{Gt\lambda}{a\sigma_{a0}}\frac{A_q}{q}\cosh q\lambda\pi/2\,. \;..\quad ..\quad ..\quad ..\quad \text{(A.III.4)}$$

The solution of these equations is

$$V_q = -\frac{4l\sigma_{a0}}{\pi^2 aEq^2}\sec\alpha\Big/\left\{\frac{1}{1+q^2\lambda^2} + \frac{\lambda q\pi\sinh q\lambda\left(\frac{\pi}{2}-\alpha\right)\cosh q\lambda\alpha}{4\cos^2\alpha\cosh q\lambda\pi/2}\right\}, \quad \text{(A.III.5)}$$

$$A_q = -\frac{\lambda a\pi\sec\alpha\, q^3 V_q}{4\cosh q\lambda\pi/2}, \quad ..\quad ..\quad ..\quad ..\quad ..\quad ..\quad ..\quad \text{(A.III.6)}$$

$$S_q = -\frac{\pi a t_s}{l\cos^2\alpha}\Big/\left\{\frac{1}{1+q^2\lambda^2} + \frac{\lambda q\pi\sinh q\lambda\left(\frac{\pi}{2}-\alpha\right)\cosh q\lambda\alpha}{4\cos^2\alpha\cosh q\lambda\pi/2}\right\}, \quad ..\quad \text{(A.III.7)}$$

$$V_0 = \frac{W(\pi/2-\alpha)\sec^2\alpha}{4Gat} + \frac{Wl^2\sec^2\alpha}{8Ea^2S_0}, \quad ..\quad ..\quad ..\quad ..\quad ..\quad \text{(A.III.8)}$$

where q takes odd positive values. For other values of q the coefficients V_q, A_q, S_q are zero.

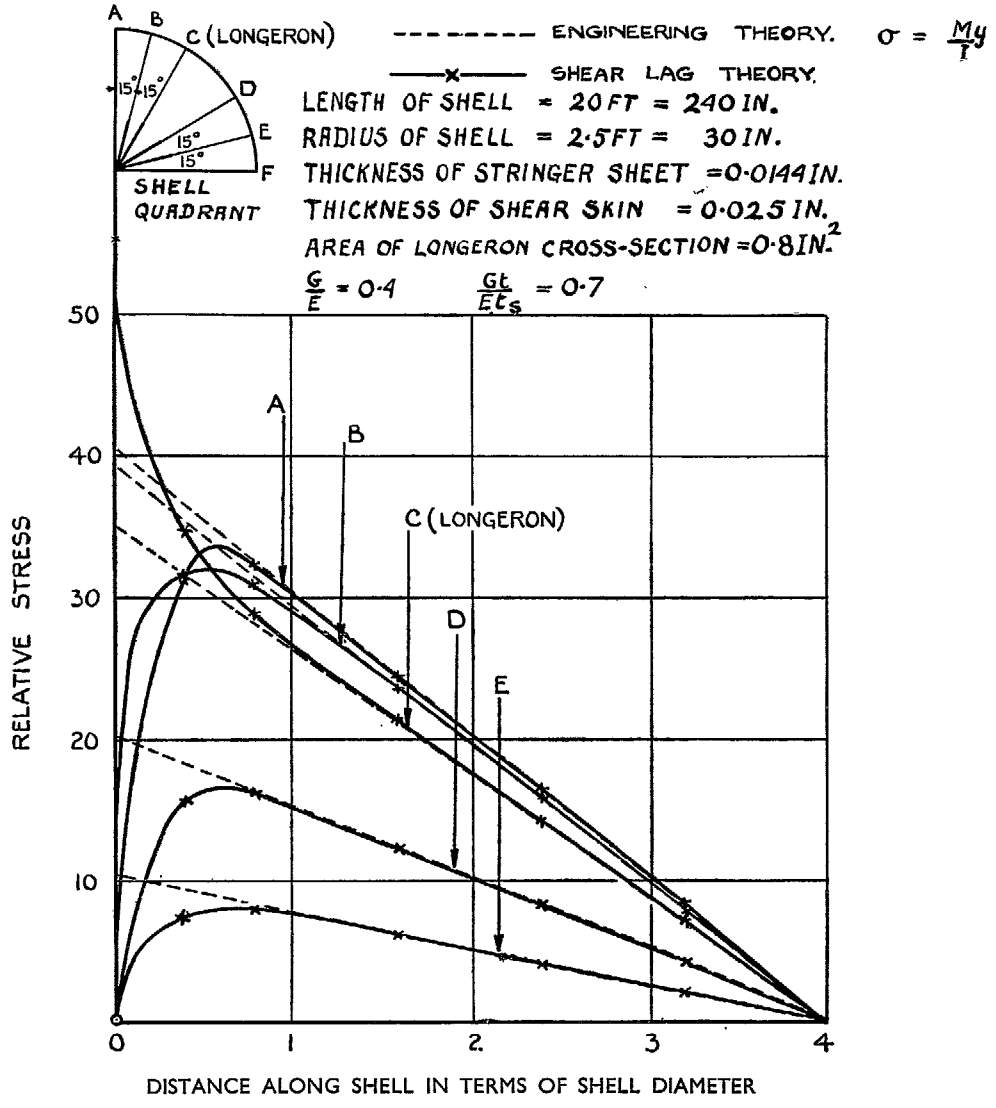

FIG. 3. Effect on Direct Axial Stresses of fixing Circular Shell at Longerons Only. (Single transverse load, uniform longerons.)

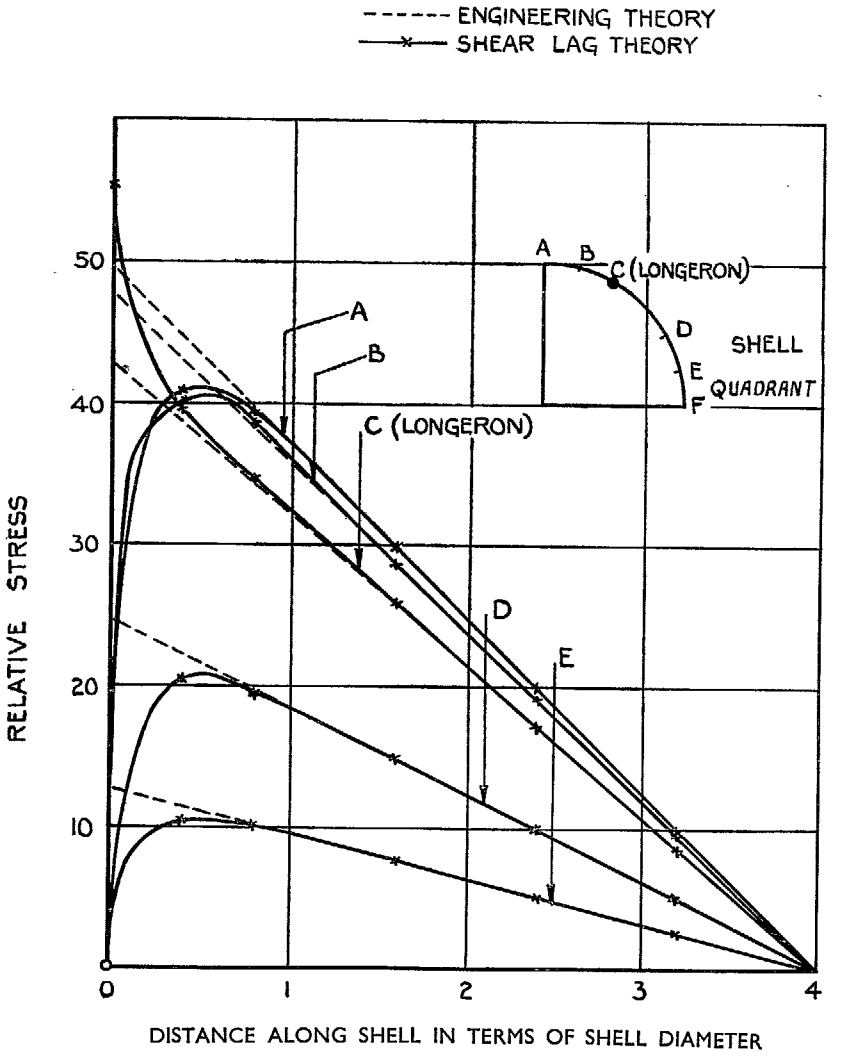

FIG. 4. Direct Axial Stresses for Shell as in Fig. 3, but with Stringer Sheet Thickness Halved

$$\left(t_s = 0{\cdot}0072 : \frac{Gt}{Et_s} = 1{\cdot}4\right)$$

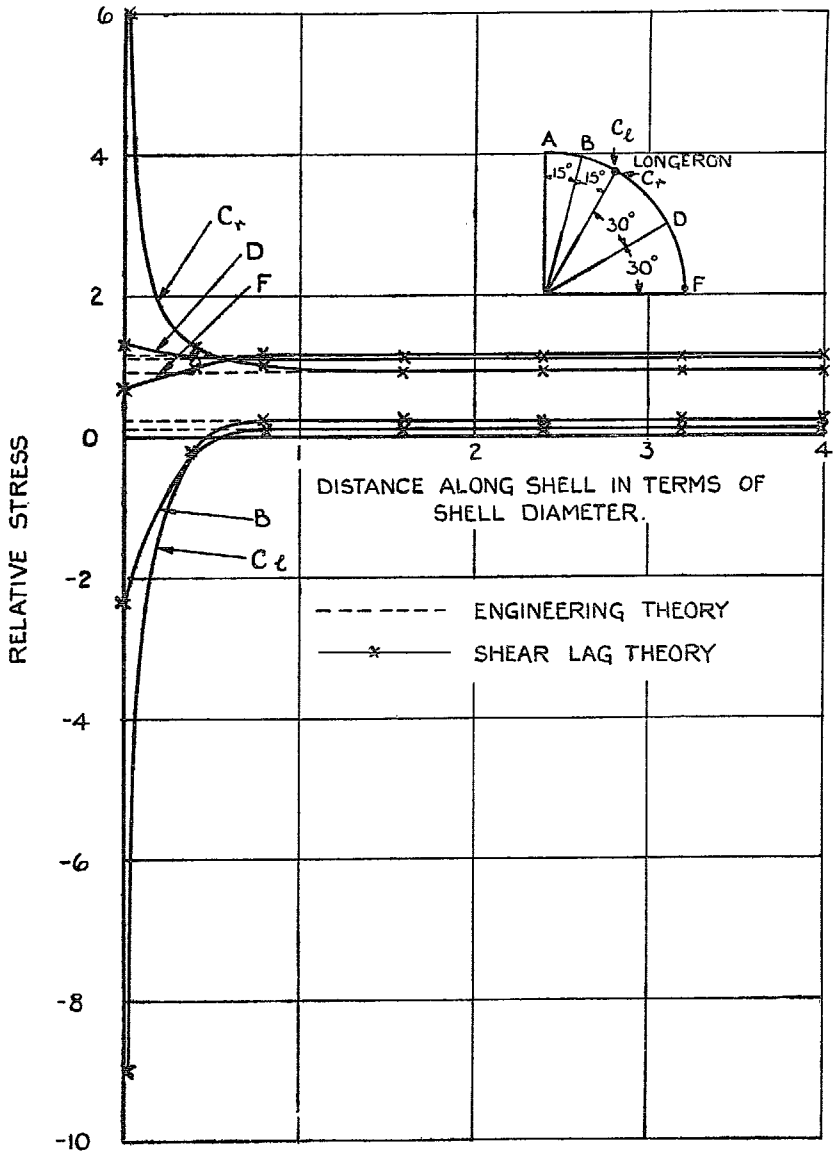

FIG. 5. Shear Stresses in Circular Shell of Fig. 3.

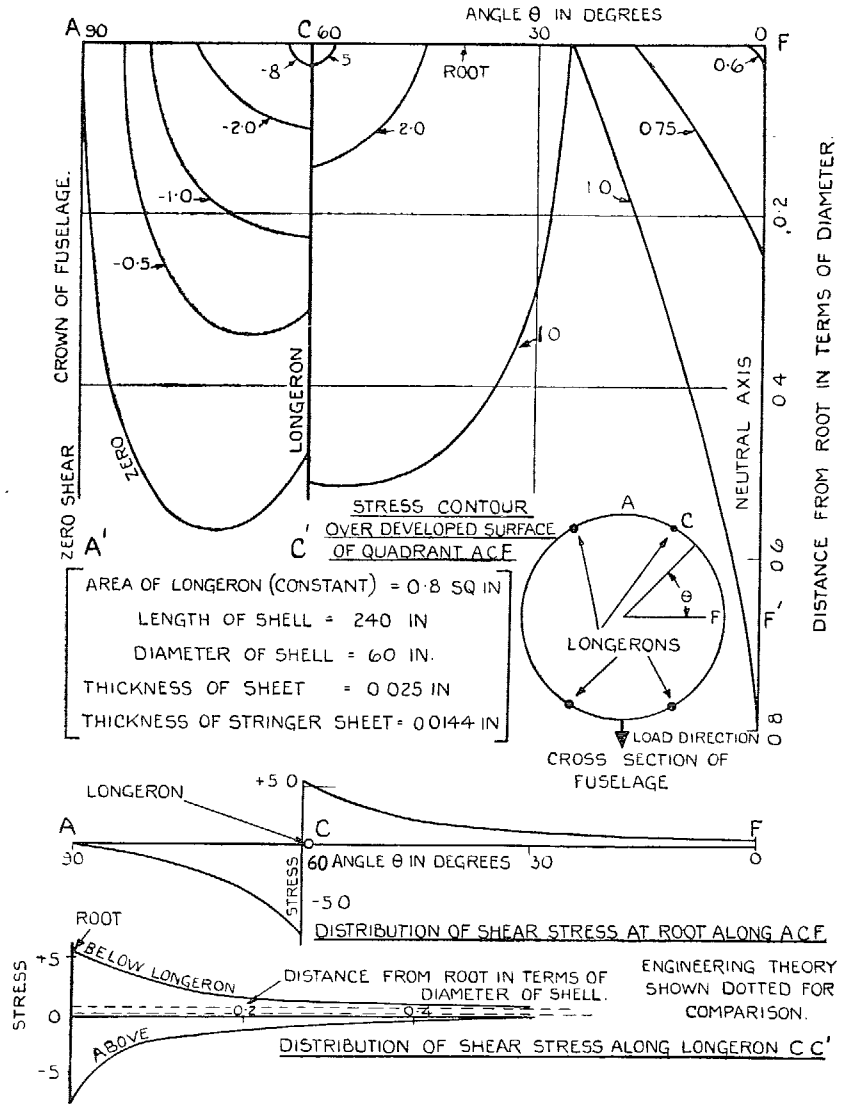

FIG. 6. Shear Stress Concentrations in a Circular-section Stressed-skin Fuselage under Transverse Loads when Root Reaction is picked up by 4 Longerons. Unit Shear Stress Represents Root Stress at the Neutral Axis on Engineering Theory.

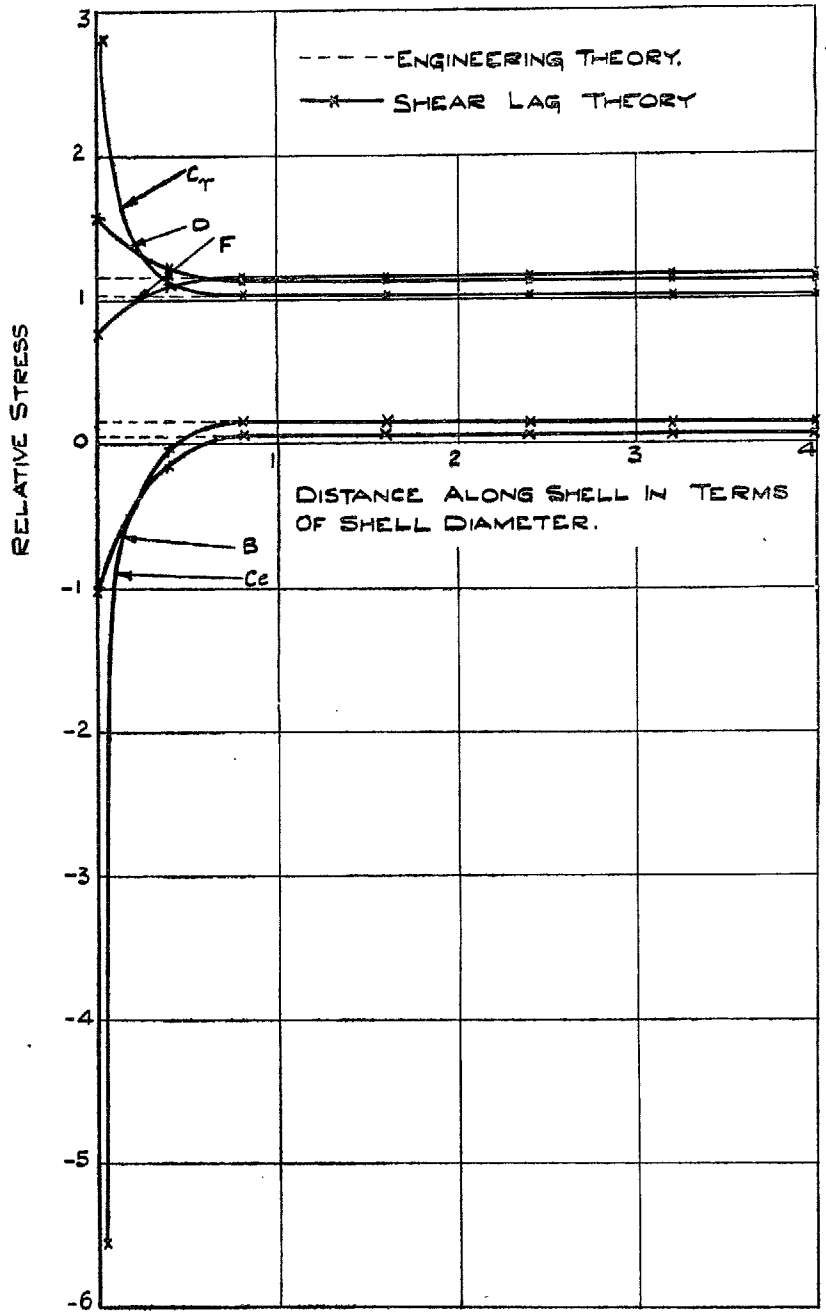

FIG. 7. Shear Stresses as in Fig. 5 but with Stringer Sheet Thickness Halved (*i.e.* Ratio Gt/Et_s Doubled).

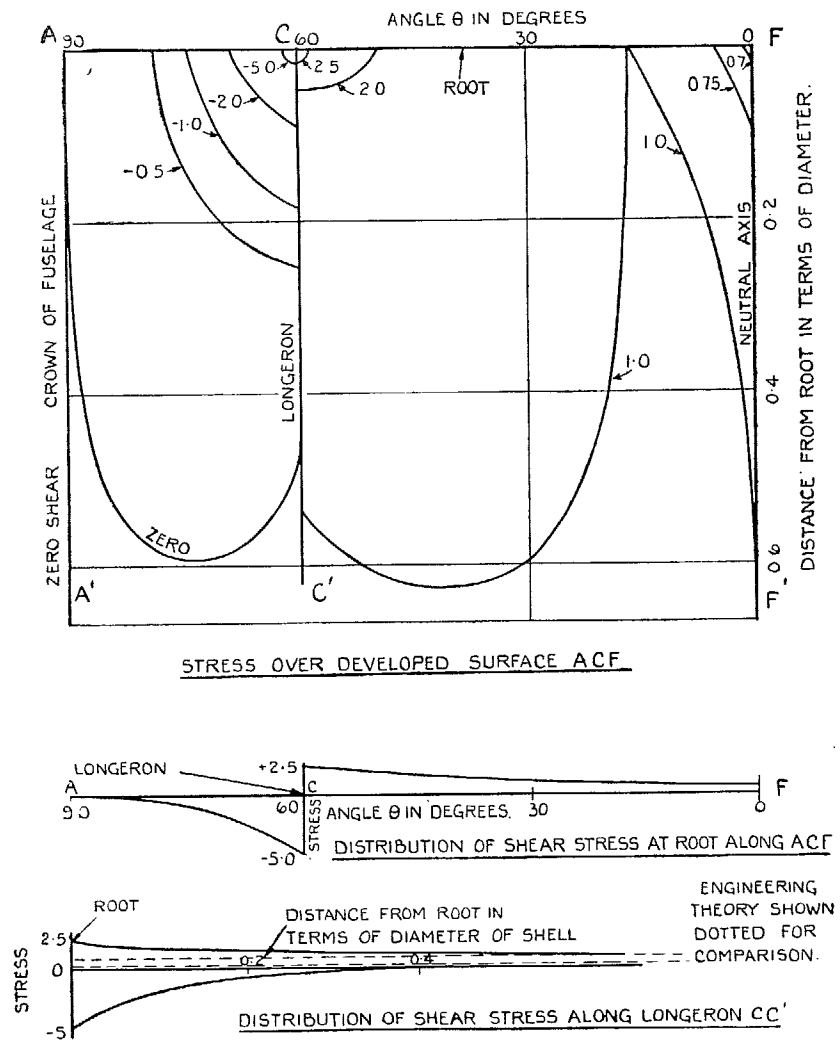

FIG. 8. As for Fig. 6 but Thickness of Stringer Sheet Halved.

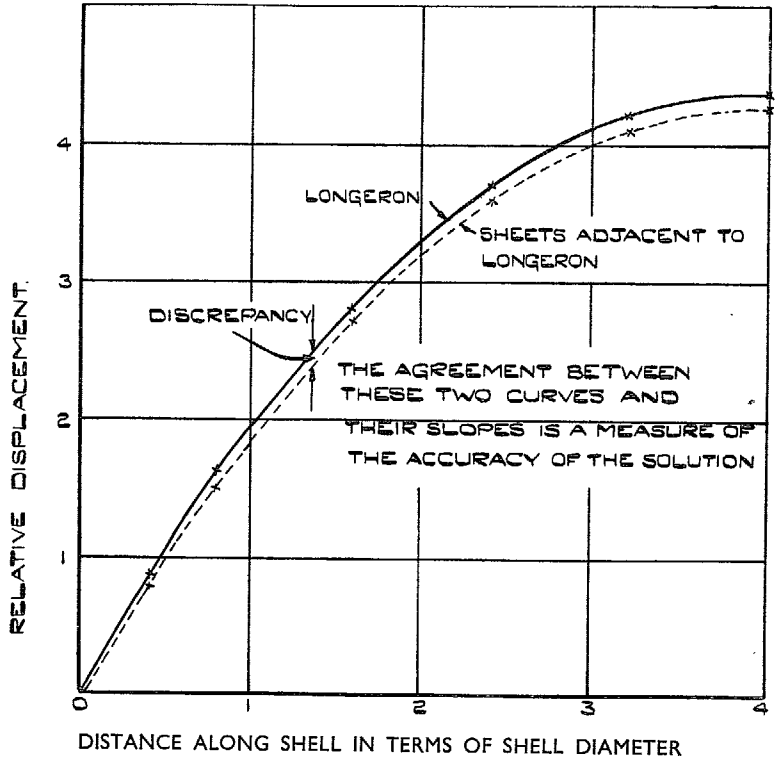

FIG. 9. Displacements of Longeron and Adjacent Sheets as given by Twenty Terms of Series ($Gt/Et_s = 1{\cdot}4$). The difference between displacements represents the discrepancy due to taking a limited number of terms.

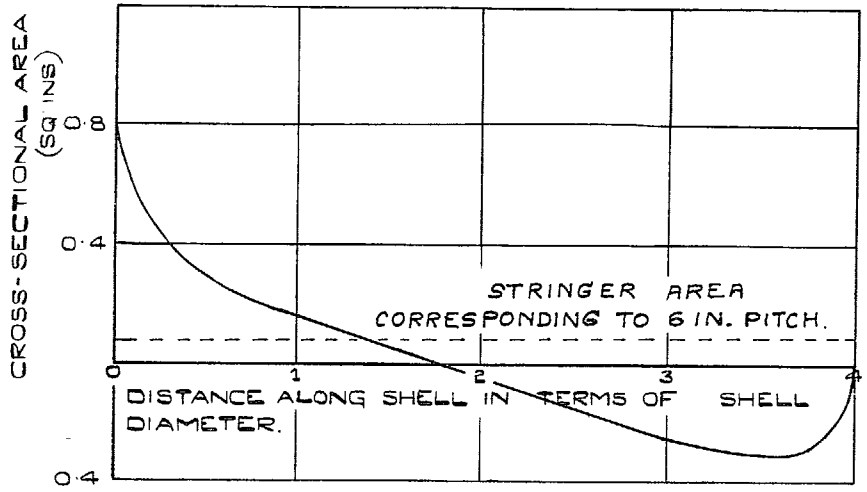

FIG. 10. Taper Necessary for Longeron of Fig. 3 in order to give Constant Stress. (Approximate method agrees with more accurate method.)

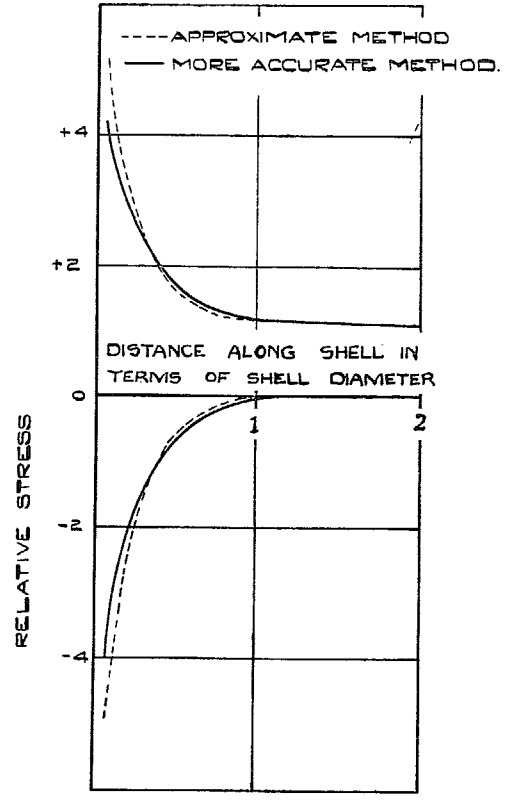

FIG. 11. Shear Stress Adjacent to Longeron. As in

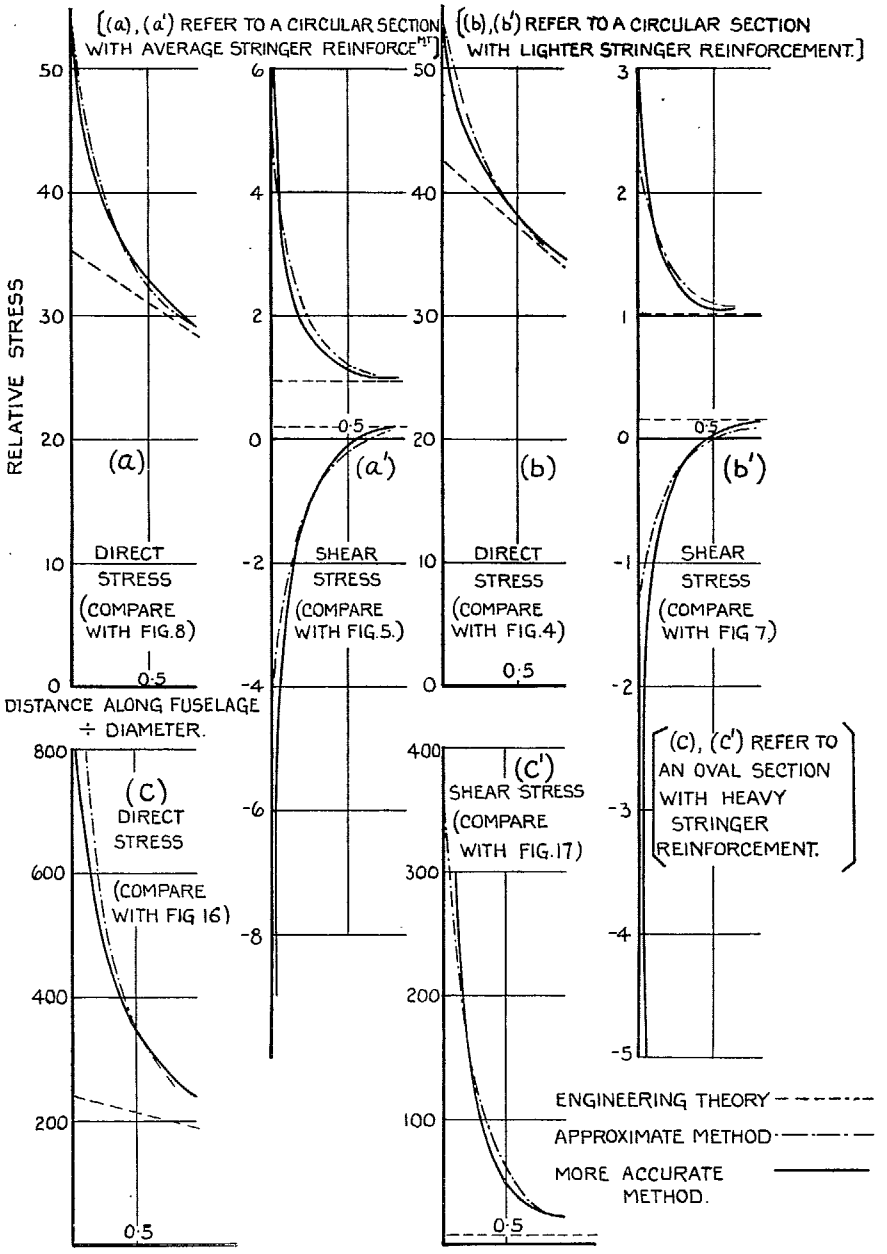

FIG. 12. Longeron Stress and Adjacent Shear Stresses as given by Engineering Theory, Approximate Method and more Accurate Method.

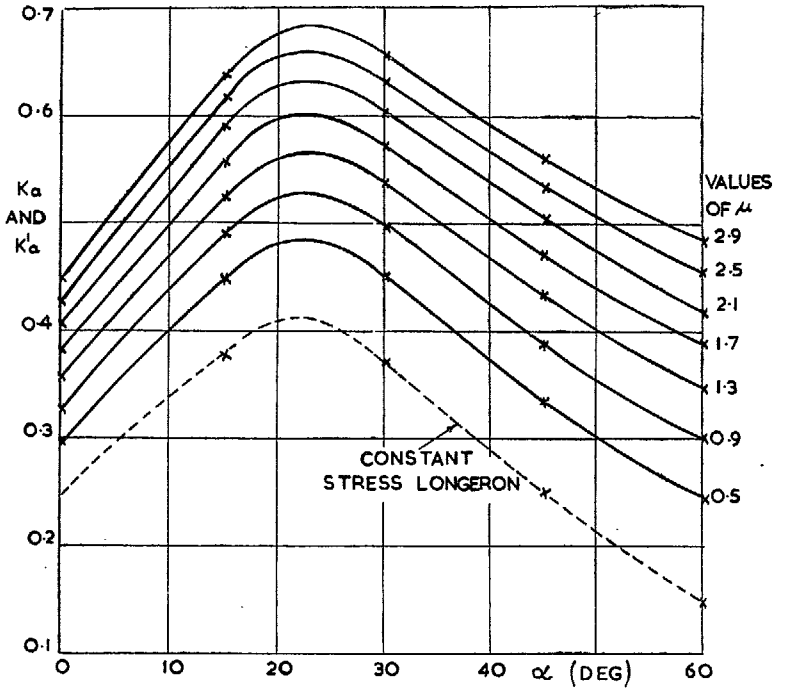

FIG. 13. Variation of ka with μ and α, and of $k'a$ with α for a Standard Section.

For other sections the method of obtaining k and k' is described in the text. (*See* § 6.6.)

(27130) Wt. 10/7116 9/47 Hw. 6372/2

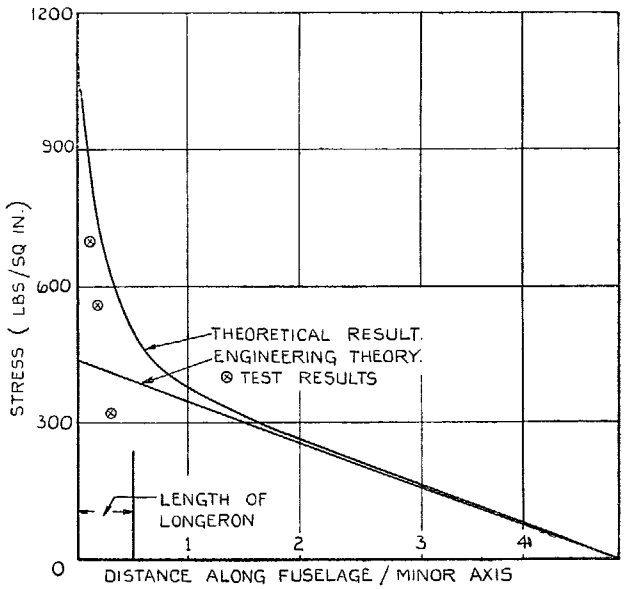

FIG. 14. Practical Case :—Direct Stress in Longeron due to Side Load of 100 lb. as given by Present Theory and by Test.
(No skin included in stringers.)

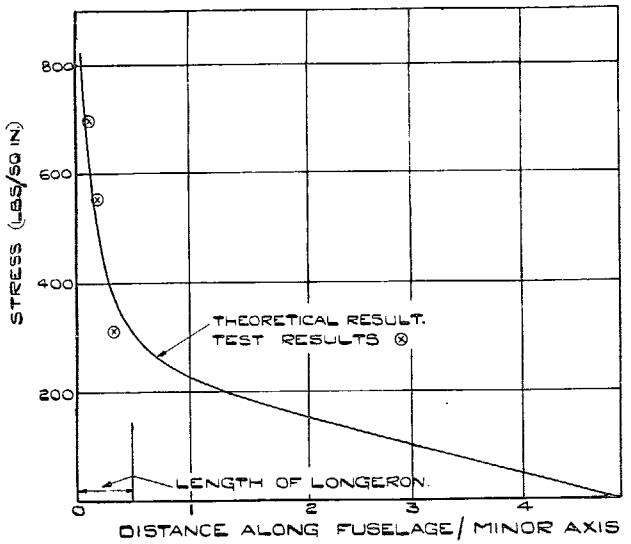

FIG. 16. Practical Case :—Direct Stress in Longeron due to Side Load of 100 lb. as given by Present Theory and by Test.
(Including all skin in stringers.)

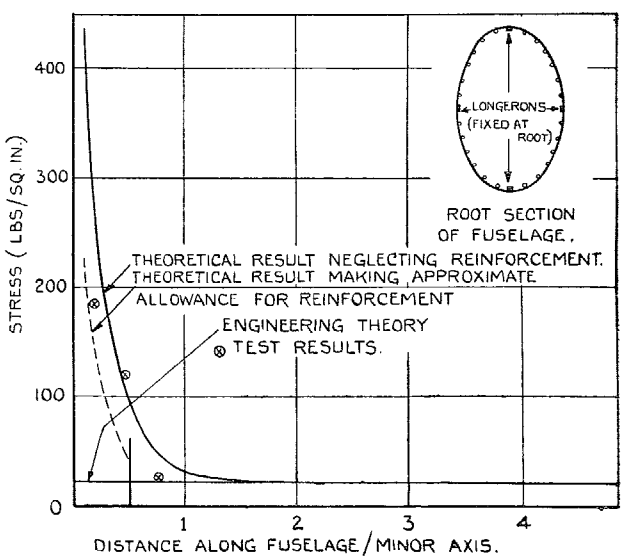

FIG. 15. Practical Case :—Shear Stress Adjacent to Longeron due to Side Load of 100 lb. as given by Present Theory and by Test.
(No skin included in stringers.)

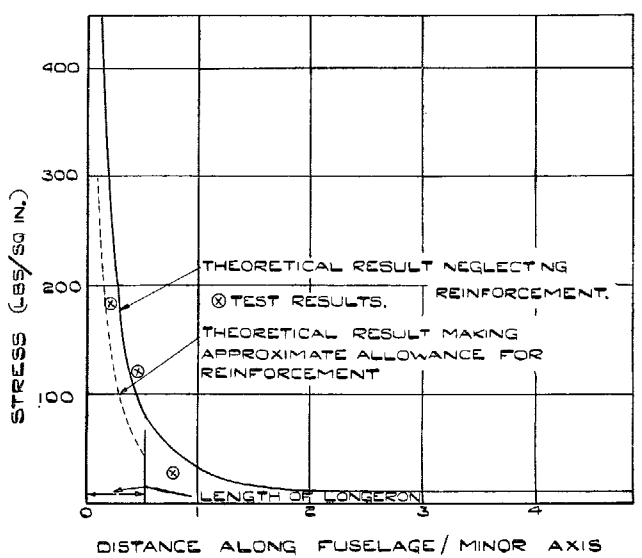

FIG. 17. Practical Case :—Shear Stress Adjacent to Longeron due to Side Load of 100 lb. as given by Present Theory and by Test.
(Including all skin in stringers.)

Publications of the Aeronautical Research Committee

TECHNICAL REPORTS OF THE AERONAUTICAL RESEARCH COMMITTEE—

1934-35 Vol. I. Aerodynamics. 40*s.* (40*s.* 8*d.*)
Vol. II. Seaplanes, Structures, Engines, Materials, etc. 40*s.* (40*s.* 8*d.*)

1935-36 Vol. I. Aerodynamics. 30*s.* (30*s.* 7*d.*)
Vol. II. Structures, Flutter, Engines, Seaplanes, etc. 30*s.* (30*s.* 7*d.*)

1936 Vol. I. Aerodynamics General, Performance, Airscrews, Flutter and Spinning. 40*s.* (40*s.* 9*d.*)
Vol. II. Stability and Control, Structures, Seaplanes, Engines, etc. 50*s.* (50*s.* 10*d.*)

1937 Vol. I. Aerodynamics General, Performance, Airscrews, Flutter and Spinning. 40*s.* (40*s.* 9*d.*)
Vol. II. Stability and Control, Structures, Seaplanes, Engines, etc. 60*s.* (61*s.*)

ANNUAL REPORTS OF THE AERONAUTICAL RESEARCH COMMITTEE—

1933-34 1*s.* 6*d.* (1*s.* 8*d.*)
1934-35 1*s.* 6*d.* (1*s.* 8*d.*)
April 1, 1935 to December 31, 1936. 4*s.* (4*s.* 4*d.*)
1937 2*s.* (2*s.* 2*d.*)
1938 1*s.* 6*d.* (1*s.* 8*d.*)

INDEXES TO THE TECHNICAL REPORTS OF THE ADVISORY COMMITTEE ON AERONAUTICS—

December 1, 1936 — June 30, 1939
Reports & Memoranda No. 1850. 1*s.* 3*d.* (1*s.* 5*d.*)

July 1, 1939 — June 30, 1945
Reports & Memoranda No. 1950. 1*s.* (1*s.* 2*d.*)

Prices in brackets include postage.

Obtainable from

His Majesty's Stationery Office

London W.C.2: York House, Kingsway
[Post Orders—P.O. Box No. 569, London, S.E.1.]
Edinburgh 2: 13A Castle Street
Manchester 2: 39-41 King Street
Cardiff: 1 St. Andrew's Crescent
Belfast: 80 Chichester Street
or through any bookseller.

S.O. Code No. 23-2100